NATIONAL ADVISORY COMMITTEE FOR AERONAUTICS

TECHNICAL NOTE 3653

SOME EFFECTS OF BLUNTNESS ON BOUNDARY-LAYER TRANSITION AND HEAT TRANSFER AT SUPERSONIC SPEEDS

By W. E. Moeckel

Lewis Flight Propulsion Laboratory
Cleveland, Ohio

Washington
March 1956

NATIONAL ADVISORY COMMITTEE FOR AERONAUTICS

TECHNICAL NOTE 3653

SOME EFFECTS OF BLUNTNESS ON BOUNDARY-LAYER TRANSITION AND HEAT TRANSFER AT SUPERSONIC SPEEDS

By W. E. Moeckel

SUMMARY

Large downstream movements of transition observed when the leading edge of a hollow cylinder or a flat plate is slightly blunted are explained in terms of the reduction in Reynolds number at the outer edge of the boundary layer due to the detached shock wave. The magnitude of this reduction is computed for cones and wedges for Mach numbers to 20. Concurrent changes in "outer-edge" Mach number and temperature are found to be in the direction that would increase the stability of the laminar boundary layer.

The hypothesis is made that transition Reynolds number is substantially unchanged when a sharp leading edge or tip is blunted. This hypothesis leads to the conclusion that the downstream movement of transition is inversely proportional to the ratio of surface Reynolds number with blunted tip or leading edge to surface Reynolds number with sharp tip or leading edge. This conclusion is in good agreement with the hollow-cylinder result at Mach 3.1.

Application of this hypothesis to other Mach numbers yields the result that blunting the tip of slender cones or the leading edge of thin wedges should produce downstream movements of transition by factors ranging from 2 at Mach 3.0 to 30 at Mach 15. The significance of this result is discussed with regard to the possible reduction in over-all heat-transfer rate and friction drag for aircraft flying at high supersonic speeds.

Mach number profiles near the surfaces of blunted cones and wedges are computed for an assumed shape of the detached shock wave at flight Mach numbers to 20. The dissipation and stability of these profiles are discussed, and a method is described for estimating the amount of blunting required to produce the maximum possible downstream movement of transition.

INTRODUCTION

In an investigation of the boundary layer on a hollow cylinder alined with the stream direction, Brinich and Diaconis discovered that the transition point moved downstream when the leading edge was slightly blunted (ref. 1). Similar results were obtained with a flat-plate wing in reference 2. A more extensive investigation of the effects of leading-edge geometry on transition (ref. 3) confirmed previous results and led directly to the explanation contained herein of the effect of blunting on transition.

When a cone or wedge is blunted slightly (sketch 1), the flow is

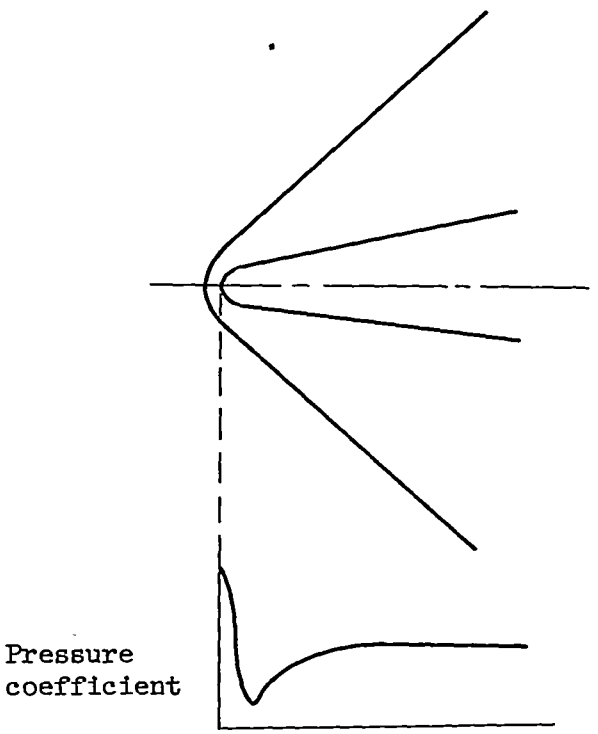

Sketch 1

changed in several ways, each of which could have a noticeable effect on the transition location. A favorable static-pressure gradient is established near the vertex which could tend to stabilize the laminar layer. Downstream of the shoulder, however, the static-pressure gradient is adverse (for moderate supersonic speeds) because of the overexpansion around the shoulder and subsequent recompression to the value corresponding to the unblunted cone or wedge. The effect of static-pressure gradient on transition is therefore inconclusive.

In addition to the static-pressure gradient along the surface, the blunting produces a stagnation-pressure gradient normal to the surface. This gradient results from the variation in stagnation-pressure loss as the detached shock decays from the normal-shock strength at the vertex to the strength corresponding to the unblunted body at some distance from the vertex. For inviscid flow, the stagnation pressure along each streamline remains constant downstream of the shock; hence, this gradient normal to the surface would persist along the entire length of the body. In the constant-static-pressure region a few bluntness diameters downstream of the vertex, the stagnation-pressure gradient results in a shear layer whose thickness depends on the size of the blunted portion of the body.

The fact that the entropy gradient produced by strongly curved shock waves might have appreciable effect on the development of the boundary layer is pointed out in references 4 and 5. Previously, the author of the present report had evaluated the shear profiles produced by detached shock waves near the surface of blunted flat plates. An explanation of the observed movement of transition in terms of these shear profiles was therefore sought.

The interaction of the boundary layer with the shear profile produced by a detached shock wave is fundamentally a very difficult analytical problem; however, the condition of most interest is one for which the interaction of the two profiles is not important. Thus, if the shear profile produced by blunting is much thicker than the boundary layer, the rate of shear of the former is negligible compared with that of the latter. The boundary layer then develops in a region of negligible shear and in a layer whose Mach number is almost constant and is less than that produced by a sharp cone or wedge.

Of particular significance is the fact that the region of reduced Mach number near the surface is also a region of reduced Reynolds number.[1] Until the boundary layer engulfs this region, its stability and transition characteristics, as well as its friction and heat-transfer characteristics, should be those associated with the reduced Reynolds number. This reduction in Reynolds number near the surface of blunted bodies explains the downstream movement of transition observed in references 1 to 3, and is the basis used in this report for comparing the boundary-layer characteristics of blunted and unblunted bodies.

---

[1]This reduction in surface Reynolds number due to blunting and its effect on laminar heating have recently been independently calculated in ref. 6 for hypersonic speeds. No attempt was made, however, to define the thickness and axial extent of the low Reynolds number layer or its effect on transition location.

ANALYSIS

The Mach number in the inviscid shear layer produced near the surface of blunted cones and wedges increases continuously from the surface value to the value that would exist at the surface of the corresponding unblunted bodies. The Reynolds number per unit length at the outer edge of the boundary layer ("outer-edge" Reynolds number) therefore remains less than the free-stream (or unblunted) value until the boundary layer absorbs the entire shock-produced shear layer. If the transition point is determined primarily by the Reynolds number at the outer edge of the boundary layer, a progressive downstream movement of transition would therefore be expected as the leading edge or tip bluntness is gradually increased. The maximum downstream movement would be expected when the blunting is sufficiently great so that the outer-edge Reynolds number is close to the inviscid surface value for the entire laminar run. In the following sections, the maximum reduction in outer-edge Reynolds number is calculated, and the blunted area required to produce this maximum reduction over the entire laminar layer is estimated.

Reduction in Surface Reynolds Number Due to Blunting

At a station sufficiently far downstream of the vertex, where the surface static pressure for a blunted body is close to that of the unblunted body, the Reynolds number near the surface can be written as

$$\frac{Re_n}{Re_1} \equiv \frac{\rho_n U_n}{\rho_1 U_1} \frac{\mu_1}{\mu_n} = \sqrt{\frac{t_1}{t_n}} \frac{M_n}{M_1} \frac{\mu_1}{\mu_n} \tag{1}$$

where subscripts n and 1 refer to inviscid surface values for the blunted and unblunted bodies, respectively. (All symbols are defined in appendix A.) These inviscid surface values will be assumed, as usual, to represent the outer-edge conditions that determine boundary-layer development.

The use of Sutherland's viscosity equation yields

$$\frac{Re_n}{Re_1} = \left(\frac{t_1}{t_n}\right)^2 \left(\frac{t_n + S}{t_1 + S}\right) \frac{M_n}{M_1} \tag{2}$$

Dividing the numerator and denominator by the ambient static temperature t_0 and converting to Mach number functions yield

$$\frac{Re_n}{Re_1} = D^2 T \frac{M_n}{M_1} \tag{3}$$

where

$$D = \frac{1 + \frac{\gamma - 1}{2} M_n^2}{1 + \frac{\gamma - 1}{2} M_1^2} \tag{4}$$

and

$$\Gamma = \frac{\frac{1 + \frac{\gamma - 1}{2} M_0^2}{1 + \frac{\gamma - 1}{2} M_n^2} + \frac{s}{t_0}}{\frac{1 + \frac{\gamma - 1}{2} M_0^2}{1 + \frac{\gamma - 1}{2} M_1^2} + \frac{s}{t_0}} \tag{5}$$

The inviscid surface Mach number for the blunted body M_n is determined by the ratio p_1/P_n, where p_1 is the static pressure at the surface of the unblunted body and P_n is the stagnation pressure downstream of a normal shock at the free-stream Mach number M_0. The inviscid surface Mach numbers are shown in figure 1 as a function of M_0 for several cone and wedge angles. Since the total pressure P_n is less than the total pressure at the surface for unblunted bodies, the surface Mach number M_n for the blunted bodies is less than the surface Mach number for the unblunted bodies M_1. The difference between M_n and M_1 increases as flight Mach number increases.

The Reynolds number ratio of equation (3) is plotted in figure 2 for the same cone and wedge angles as those in figure 1. This ratio decreases rapidly as flight Mach number increases. If the transition Reynolds number is unchanged when the leading edge or tip is blunted, and if the blunting is adequate to cover the laminar boundary layer with a sufficiently thick layer of low Reynolds number air, then it should be possible to increase the length of laminar run by a factor inversely proportional to the Reynolds number ratio of figure 2. For slender cones and wedges, the possible increases in laminar run range from factors of the order of 2.0 at $M_0 = 3.0$ to 10 at $M_0 = 8.0$ and 30 at $M_0 = 15.0$. The significance of such large increases in laminar run for reducing the heat-transfer rate and friction drag for very high-speed aircraft is apparent.

Evidence that increases in laminar run of the magnitude indicated by figure 2 are actually attainable is presented in references 1 to 3.

In reference 3, for example, the transition point at $M_0 = 3.1$ was moved downstream by a factor of 2 (from 5 to 10 in. at a Reynolds number of 3.56×10^5/in.) when the leading-edge thickness was increased from 0.0008 to 0.008 inch. This experimental movement of transition compares very favorably with the value 2.17 predicted on the basis of the Reynolds number reduction shown in figure 2(b).

In reference 2, downstream movements by factors ranging from 2.3 to 3.6 were observed for a blunted flat plate at various angles of attack at $M_0 = 4.04$. The movement predicted by figure 2(b) for this Mach number is 3.57. For swept wings, little or no downstream movement was observed in reference 2. This is in agreement with the expected weakening of the leading-edge shock due to sweepback. Whether downstream movements of the order of magnitude predicted by figure 2 are attainable at higher Mach number or for other body shapes remains to be established by further experiments.

Estimation of Bluntness Required to Obtain Maximum Movement of Transition

In order to determine the bluntness area required to cover the entire laminar boundary layer with a low Reynolds number layer of negligible gradient, it is convenient to define a thickness of this layer which limits the Mach number to values near the inviscid surface value. A suitable thickness is the distance from the surface to the streamline that passes through the sonic point of the detached shock wave (point where the Mach number just behind the shock is unity). From the vertex to the sonic point the stagnation pressure downstream of the shock does not vary greatly; consequently, the Mach number should remain near the inviscid surface value in the layer thus defined.

An expression for the thickness will be derived under the assumption that the shear profile produced by the detached shock does not diffuse or dissipate, that is, the profile remains unchanged until it is engulfed by the boundary layer. The rate of dissipation of the shock-produced shear layer is discussed in appendix B, and tends to increase the bluntness area required to produce a given thickness of the low Mach number layer.

With dissipation neglected, the thickness of the low Mach number region can be estimated by means of the detached-shock-wave theory of reference 7. In this theory, the detached shock wave is assumed to have a hyperbolic form independent of the shape of the body that produces it. This form has been found to agree well with experimental results for a large range of body shapes in the moderate supersonic Mach

number range (ref. 8), but becomes more questionable as the Mach number increases. The portion of the shock from the vertex to the sonic point, however, can be satisfactorily represented by the assumed hyperbola for all Mach numbers. This form of the shock wave should, therefore, yield a satisfactory estimate of the thickness of the low Mach number layer as well as the shock location, to the extent that the other assumptions of the theory (constant specific heat, inviscid flow, etc.) are valid.

In order to estimate this thickness, the Mach number in the layer is assumed to be constant at a value corresponding to the mass centroid of the layer. This Mach number, denoted by M_C, is determined from the ratio p_1/P_C, where p_1 is the static pressure on the surface of the unblunted cone or wedge and P_C is the total pressure downstream of the shock on the centroid streamline. (A simple and satisfactory estimate of P_C can be obtained by using the arithmetic mean of the stagnation pressures at the sonic point and at the vertex.) The continuity equation for the layer shown in sketch 2 can be written

$$P_C A_n (A^*/A)_{M_C} = P_O A_S (A^*/A)_{M_O} \tag{6}$$

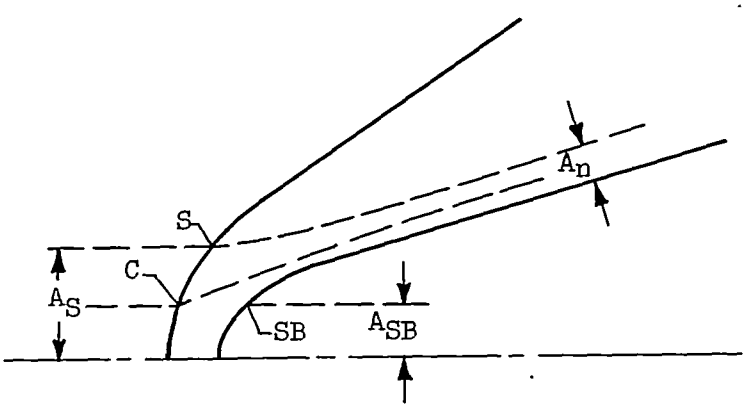

Sketch 2

where A_n is the area of the low Mach number layer and A_S is the free-stream area of the stream tube between the axis and the shock sonic point S. If the bluntness of the body is defined as its cross-sectional area at the sonic point A_{SB} (sketch 2), the ratio of the area of the low Mach number layer to the blunted area becomes

$$\frac{A_n}{A_{SB}} = \frac{A_S}{A_{SB}} \frac{P_O}{P_C} \frac{(A^*/A)_{M_O}}{(A^*/A)_{M_C}} \tag{7}$$

From reference 7,

$$\frac{A_S}{A_{SB}} = \frac{1}{1 - B \cos \eta} \tag{8}$$

where $B = \frac{P_0}{P_C} (A^*/A)_{M_0}$, and η is the mean inclination of the sonic line defined in reference 7.

The area of the low Mach number layer defined by equation (7) is shown in figure 3. This area is seen to increase rapidly with increasing Mach numbers for the blunted flat plate ($\theta_W = 0$) and for the blunt-nosed cylinder ($\theta_c = 0$). However, for wedge half-angles greater than 5° and cone half-angles greater than 10°, the area does not vary greatly with Mach number.

With the thickness of the low Mach number and low Reynolds number layer thus defined, the blunting required to provide a low external-stream Reynolds number for the entire laminar boundary layer to the expected or hoped-for transition point can be estimated. This is done by calculating the laminar boundary-layer thickness at the expected transition Reynolds number, which is based on conditions in the low Mach number layer near the surface. By equating this thickness to the thickness of the low Reynolds number layer, the required values of the bluntness area can be calculated.

Thus, for blunted wedges the required ordinate at the body sonic point is

$$y_{SB} = \frac{\delta_{tr}}{(A_n/A_{SB})} \tag{9}$$

while for blunted cones (with $\delta_{tr} \ll r_1$),

$$y_{SB} = \left[\frac{2r_{1,tr}\delta_{tr}}{(A_n/A_{SB})}\right]^{1/2} \tag{10}$$

where A_n/A_{SB} is given in figure 3, and $r_{1,tr}$ is the radius of the blunted cone at the expected transition point. Equations (9) and (10) show that the amount of blunting required to cover the laminar boundary layer with a low Reynolds number layer is not large. For the wedge (eq. (9)), the ordinate of the body at the sonic point need be only of the order of magnitude of the boundary-layer thickness at the expected transition point; for the cone (eq. (10)), the required radius of the

body at the sonic point is of the order of the geometric mean of the body radius and the boundary-layer thickness at the expected transition point.

The required bluntness is considerably reduced if the displacement effect is considered, since the low Reynolds number layer is moved away from the surface by an amount equal to the displacement thickness of the boundary layer (ref. 3). The required values of y_{SB} should therefore be calculated with $(\delta - \delta^*)_{tr}$ in place of δ_{tr} in equations (9) and (10). Expressions for δ and δ^* for constant surface temperature were obtained from equations (18) and (22) of reference 9, based on the flat-plate theory of reference 10. The value of δ was assumed to correspond to $\frac{u}{u_\infty} = 0.99$. At the transition point, these expressions can be combined to yield (for $\gamma = 1.40$)

$$\left(\frac{\delta}{L}\right)_{tr} - \left(\frac{\delta^*}{L}\right)_{tr} = 3.48\sqrt{\frac{C}{Re_{tr}}} \tag{11}$$

where L_{tr} is the distance along the surface to the transition point and C is the proportionality constant in the linear viscosity-temperature variation. For cones, this expression is divided by $\sqrt{3}$. In terms of $(\delta - \delta^*)_{tr}$, the bluntness required to cover the laminar boundary layer with a low Reynolds number layer becomes

$$\frac{y_{SB}}{L_{tr}} = \frac{(\delta/L)_{tr} - (\delta^*/L)_{tr}}{(A_n/A_{SB})} \tag{12}$$

for wedges and

$$\frac{y_{SB}}{L_{tr}} = \left\{\frac{\frac{2}{\sqrt{3}}\left(\frac{r_1}{L}\right)_{tr}\left[\left(\frac{\delta}{L}\right)_{tr} - \left(\frac{\delta^*}{L}\right)_{tr}\right]}{(A_n/A_{SB})}\right\}^{1/2} \tag{13}$$

for cones.

With equation (12), the calculated bluntness areas agree as closely as could be expected with the experimental values that produced the maximum downstream movement of transition in the experiments of reference 3. This maximum downstream movement was found to take place for a leading-edge thickness of about 0.008 inch, which is about two-thirds of the calculated value. Further increases in leading-edge thickness had no appreciable effect on transition location. Since the thickness

of the low Reynolds number layer has been rather arbitrarily defined, the values of y_{SB} calculated from equations (12) and (13) can be regarded only as rough estimates of the blunting required to produce maximum downstream movement of transition. These values should, however, be on the conservative side, since they produce nearly the maximum possible reduction in Reynolds number and Mach number over the entire laminar boundary layer.

Inviscid Mach Number Profiles for Blunted Cones and Wedges

Although the maximum effect of blunting on boundary-layer development and transition depends on the portion of the shock-produced shear layer near the surface, the entire shear profile is of interest if the outer edge of the boundary layer moves out of the low Reynolds number layer defined in the preceding section. In order to determine the nature of the entire shock-produced shear profile, the shape and location of the shock must be prescribed. For moderate supersonic speeds, the hyperbolic form assumed in reference 7 is adequate; but as the flight speed approaches the hypersonic range, the portion of the shock beyond the sonic point is increasingly influenced by body shape. This situation arises partly because the region between the shock and the body becomes smaller as M_0 increases; consequently, characteristics from portions of the body far downstream of the sonic point reach the shock before it has decayed to its asymptotic strength. In addition, the overexpansion near the shoulder of slender blunted bodies, which takes place at lower speeds, gradually becomes an underexpansion at hypersonic speeds, that is, a Prandtl-Meyer expansion from the sonic point fails to reduce the pressure to, or below, the asymptotic static pressure. A rather long process of reflection of expansion waves between the shock and the body must, therefore, take place before the asymptotic pressure is reached on blunted cones or wedges.

This consideration also affects the distance required to obtain the inviscid surface Mach numbers and Reynolds numbers calculated in the preceding sections. A more accurate evaluation of the effect of blunting would include the variation of outer-edge Mach number and Reynolds number along the entire body due to the pressure gradient. Perhaps mean values of these numbers could be used to predict the location of transition. These mean values would be lower than those shown in figures 1 and 2, which means that the predicted transition point would be even farther downstream than if the pressure gradient is neglected. The fact that the self-induced pressure gradient is entirely favorable also tends to increase the stability of the laminar layer. The effect on transition of increasing flight Mach number thus appears to be a favorable one. For computing the shock-produced shear profile, however, the narrowing region between shock and body as flight speed

increases introduces difficulties, in that no general shock shape is available beyond the sonic point, and the asymptotic profile may be so far downstream as to have no practical significance. It was nevertheless felt to be worthwhile to compute these asymptotic profiles for very high M_0 with the hyperbolic shock form of reference 7, if only for comparison with more accurate future computations based on experimented shock forms or exact characteristic solutions for particular bodies. The variation with Mach number of the hyperbolic shock of reference 7 is similar to that which would be expected, in that it decays much more slowly for hypersonic speeds than for moderate supersonic speeds.

The computation method is presented in appendix C, and the resulting asymptotic inviscid shear profiles are shown in figure 4 for flight Mach numbers from 2 to 20. Indicated on each profile is the thickness of the low Mach number layer as defined in the preceding section. It is seen that this definition does, in fact, restrict the Mach number to values close to the surface value.

The profiles for blunted wedges differ qualitatively from those of blunted cones at all Mach numbers. For the blunted wedges, the Mach number gradient is zero at the surface; whereas, for blunted cones the gradient has a positive value. Since these gradients depend on the form of the shock near its vertex, they should be correct for all Mach numbers within the limitations of the other assumptions of the analysis (static pressure equal to values for the unblunted body, constant specific heat, inviscid flow, etc.). The portions of the profiles above the boundary of the low Mach number layer should be good approximations for M_0 less than 5.0, but seem to become much too thick at higher Mach numbers, particularly for the flat plate ($\theta_w = 0$) and for the blunt-nosed cylinder ($\theta_c = 0$). This thickness is associated with the very slow decay rate of the assumed hyperbolic shock at these Mach numbers. Since the shock lies quite close to the body at hypersonic speeds, these profiles would, as previously surmised, be applicable, if at all, only at very large distances from the vertex, where the shear layer is thin compared with the distance from the surface to the shock wave. At such distances, of course, the boundary layer, which is of the same order of thickness as the layer between the shock and the body at hypersonic speeds, would already have engulfed the entire shock-produced shear layer.

For higher cone and wedge angles, the shock decays more rapidly to the asymptotic strength, and the resulting profiles appear to be more in harmony with expectations.

Although the computed profiles beyond the boundary of the low Reynolds number layer are not reliable at high Mach numbers, they agree well with measured profiles at Mach 3.1 (ref. 3). If more accurate

shock-produced profiles are desired for higher speeds, the shock form must be calculated for each body shape. Such computations would be useful for estimating the variation of transition location as the blunted area is gradually increased, but are not required for estimating the maximum downstream movement, or the blunted area required to produce this movement.

Changes in Laminar Recovery Temperature, Heat-Transfer Rate, and Friction Coefficient

The downstream movement of transition due to blunting means that larger portions of the aircraft surfaces will be subjected to laminar, rather than turbulent, heat-transfer rates and friction coefficients. The blunting should, therefore, produce substantial reductions in overall heat-transfer rate and friction drag. There is, however, an increase in laminar equilibrium recovery temperature corresponding to the reduction in Mach number, and a change in laminar heat-transfer rate and friction coefficient due to the reduction in Reynolds number. These must be evaluated in order to estimate the magnitude of the advantages due to blunting.

The heat-transfer coefficient and friction-drag equations of reference 11 are used for this estimate. Although these equations are based on the assumptions of constant specific heat and Prandtl number, and no dissociation, they agree in order of magnitude with more exact numerical computations even at hypersonic speeds (ref. 12).

The ratio of laminar heat-transfer rate with and without blunting can be written

$$\frac{q_n}{q_1} \equiv \frac{h_n}{h_1}\left(\frac{t_{e,n} - t_w}{t_{e,1} - t_w}\right) = \frac{\sqrt{M_n/M_1}}{\sqrt{D\Gamma}} \quad \frac{g^*\left(0,\frac{t_w}{t_n},M_n\right)}{g^*\left(0,\frac{t_w}{t_1},M_1\right)}\left(\frac{t_{e,n} - t_w}{t_{e,1} - t_w}\right) \tag{14}$$

where D and Γ are defined by equations (4) and (5), $t_{e,n}$ and $t_{e,1}$ are equilibrium recovery temperatures with and without blunting, and $g^*\left(0,\frac{t_w}{t_\infty},M_\infty\right)$ is the shear function of reference 11 evaluated at the surface. This function is given in reference 11 for several outer-edge Mach numbers M_∞ and several ratios of surface temperature to outer-edge temperature t_w/t_∞.

The temperature-difference ratio in equation (14) can be written

$$\frac{t_{e,n} - t_w}{t_{e,l} - t_w} = \frac{\frac{t_n}{t_0}\left[1 + 0.845\left(\frac{\gamma - 1}{2}\right)M_n^2\right] - \frac{t_w}{t_0}}{\frac{t_l}{t_0}\left[1 + 0.845\left(\frac{\gamma - 1}{2}\right)M_l^2\right] - \frac{t_w}{t_0}} = \frac{\frac{1 + 0.2M_0^2}{1 + 0.2M_n^2}\left(1 + 0.169M_n^2\right) - \frac{t_w}{t_0}}{\frac{1 + 0.2M_0^2}{1 + 0.2M_l^2}\left(1 + 0.169M_l^2\right) - \frac{t_w}{t_0}} \tag{15}$$

where the laminar recovery factor is assumed to be 0.845 and γ is 1.4.

The ratio of equilibrium surface temperatures with and without blunting is obtained from the definition of recovery factor:

$$\frac{t_{e,n} - t_n}{T_0 - t_n} = \frac{t_{e,l} - t_l}{T_0 - t_l} = 0.845 \tag{16}$$

whence

$$\frac{t_{e,n}}{t_{e,l}} = \frac{\frac{0.155}{1 + 0.2M_n^2} + 0.845}{\frac{0.155}{1 + 0.2M_l^2} + 0.845} \tag{17}$$

The laminar-skin-friction ratio is, from the equations of reference 11,

$$\frac{\tau_{w,n}}{\tau_{w,l}} = \frac{(M_n/M_l)^{3/2}}{D\sqrt{\Gamma}} \frac{g^*\left(0, \frac{t_w}{t_n}, M_n\right)}{g^*\left(0, \frac{t_w}{t_l}, M_l\right)} = \frac{\frac{M_n}{M_l}\frac{h_n}{h_l}}{\sqrt{D}} \tag{18}$$

The ratios of laminar recovery temperature, skin friction, and heat transfer for flat plates are shown in figure 5. Although there is a slight increase in laminar equilibrium temperature for the blunted flat plate (this was observed experimentally in ref. 3), the laminar skin friction is reduced over the entire range of flight Mach numbers, and the heat-transfer rate is reduced except for wall temperature near equilibrium. (The rapid increase in the heat-transfer ratio near recovery temperature arises from the small increase in recovery temperature due to blunting. The heat transfer without blunting approaches zero

for these values, whereas the heat transfer with blunting becomes small but is not yet zero.) Figure 5 shows that blunting the leading edge of a flat plate or cylinder can produce, in addition to the longer laminar run, a small but significant reduction in the skin friction and heat-transfer rate of the laminar boundary layer itself.

Cooling Requirements for Stability

The static temperature at the edge of the boundary layer is considerably higher for a blunted cone or wedge than for sharp bodies. The ratio t_n/t_l is, in fact, given by $1/D$ (eq. (4)). This increase in outer-edge temperature means that, for a given surface temperature t_w, the ratio t_w/t_n is smaller than t_w/t_l. The outer-edge Mach number is also reduced. Shown in figure 6 are the outer-edge conditions for a blunted and unblunted flat plate, and for a blunted and unblunted 10° half-angle cone for a surface-to-ambient temperature ratio of 4.0. These conditions are compared with two of the laminar stability limits given in references 12 and 13. This comparison shows that blunting moves the outer-edge conditions far into the stable region in the hypersonic speed range. (Although the stability-range curves shown are based on two-dimensional disturbance theory, recent computations by Dunn and Lin (ref. 13) indicate that three-dimensional disturbance theory also yields laminar stability to extremely high Reynolds number but that somewhat lower surface temperatures are required.)

3880

Effect of Blunting on Heat-Transfer Rate Near the Nose

In order to estimate more accurately the net decrease in heat-transfer rate due to blunting, it is necessary to determine how the heat-transfer rate near the nose of the blunted cone differs from that on the pointed cone. An estimate of this difference can be made by comparing the heat-transfer rate for the sharp conical nose with that for the inscribed spherical nose (sketch 3).

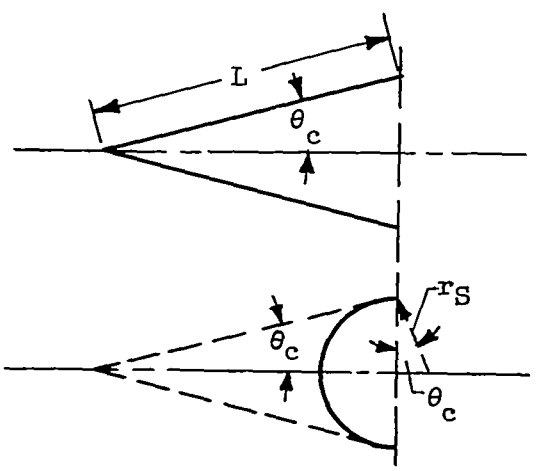

Sketch 3

This heat-transfer ratio can be written as

$$\frac{q_{sp}}{q_c} = \frac{h_{sp}}{h_c} \frac{A_{sp}}{A_c} \frac{(T_0 - t_w)}{(T_{e,1} - t_w)} \tag{19}$$

where the subscripts sp and c refer to the spherical and conical nose, respectively. The area ratio of equation (19) is

$$\frac{A_{sp}}{A_c} = 2 \frac{\tan \theta_c}{\cos \theta_c} (1 - \sin \theta_c) \tag{20}$$

and the temperature-difference ratio is

$$\frac{T_0 - t_w}{T_{e,1} - t_w} = \frac{1 + \frac{\gamma - 1}{2} M_0^2 - \frac{t_w}{t_0}}{\frac{1 + \frac{\gamma - 1}{2} M_0^2}{1 + \frac{\gamma - 1}{2} M_1^2} \left(1 + \frac{\gamma - 1}{2} r M_1^2\right) - \frac{t_w}{t_0}} \tag{21}$$

The mean heat-transfer coefficient for the spherical nose is assumed to be the stagnation-point value presented in reference 14:

$$h_{sp} = k_w \sqrt{\frac{c}{\nu_w}} \left(\frac{Nu}{\sqrt{Re_w}}\right)_{sp} \tag{22}$$

where $c = \frac{U_0}{r} \sqrt{\frac{\rho_0}{\rho_{st}} C_{p,st}}$ and $(Nu/\sqrt{Re_w})_{sp}$ is about 0.61 for a Prandtl number of 0.72 and for a ratio of wall temperature to stagnation temperature (t_w/T_0) close to zero (corresponding to cooled surfaces at very high M_0).[2] The stagnation pressure coefficient $C_{p,st}$ is 1.84 for $\gamma = 1.4$. The mean cone heat-transfer coefficient is, from reference (14),

$$h_c = \frac{4}{3} \left(\frac{Nu}{\sqrt{Re_w}}\right)_c \frac{k_w}{\sqrt{\nu_w}} \sqrt{\frac{U_{1,c}}{L}} \tag{23}$$

[2]Since the publication of ref. 14, Reshotko and Cohen have found that the expression for c given therein for supersonic flow is in error. The correct expression for this constant is that given above.

where $\left(\mathrm{Nu}/\sqrt{\mathrm{Re_w}}\right)_c$ is 0.51. The ratio of heat-transfer coefficients, therefore, becomes

$$\frac{h_{sp}}{h_c} = \frac{\left(\frac{\mathrm{Nu}}{\sqrt{\mathrm{Re_w}}}\right)_{sp}}{\frac{4}{3}\left(\frac{\mathrm{Nu}}{\sqrt{\mathrm{Re_w}}}\right)_c}\left(\frac{M_0}{M_1}\cot\theta_c\sqrt{C_{p,st}\frac{T_0}{t_1}\frac{p_0}{P_{st}}}\right)^{1/2} \tag{24}$$

where P_{st} is the stagnation pressure behind a normal shock at Mach number M_0. The heat transfer ratio obtained by substituting equations (20), (21), and (24) into equation (19) is plotted in figure 7 for cone half-angles of 10° and 20° and for a surface-to-ambient static-temperature ratio of 1.0. The over-all heat transfer for the inscribed spherical nose is seen to be less than half as great as that for the conical nose. The blunted nose, therefore, has the advantage of a lower heat-transfer rate near the vertex as well as along the downstream surfaces.

3880

DISCUSSION

The preceding sections have shown that the Reynolds number per unit length at the outer edge of the boundary layer is lower for blunted fuselages and wings than for unblunted ones. The limited data available agree with the conclusion that the transition location can be increased by a factor of the order of the ratio of the surface Reynolds number without blunting to the surface Reynolds number with blunting. This factor increases rapidly with increased flight speed, particularly for moderately slender wings and bodies.

As an example of the magnitude of this effect, a 10° half-angle cone at a Mach number of 15 will be considered. If the transition point is located 1 foot downstream of the vertex without blunting, it might, on the basis of figure 2, be moved 25 feet downstream of the vertex if the tip is blunted.

The bluntness required is, from equations (11) and (13),

$$\frac{y_{SB}}{L_{tr}} = 0.5\left(\frac{C}{\mathrm{Re_{tr}}}\right)^{1/4}$$

If $\left(\frac{C}{\mathrm{Re_{tr}}}\right)$ is of the order of 10^{-6}, then the required value for y_{SB} is only about 5 inches. The ratio of the blunted area to the cross-sectional area of the cone at the transition point is, therefore, approximately 0.01. If the transition point (25 ft) is near the end of the body, the

over-all heat-transfer rate would be reduced by blunting from the value corresponding to almost completely turbulent flow to the value corresponding to completely laminar flow. The blunted cone would, therefore, heat up much more slowly than the pointed cone and would require much less coolant to maintain a given surface temperature. The ratio L_{tr}/y_n is about 300; therefore, the effect of dissipation of the shock-produced shear layer can probably be neglected (see appendix B).

Furthermore, during the heating process the ratio of surface temperature to outer-edge temperature remains much lower for the blunted cone or wedge (fig. 6) so that the advantages of cooled surfaces with regard to laminar stability prevail longer than for the pointed cone or sharp-edged wedges. Both the low surface Reynolds number and the higher outer-edge temperatures work toward preservation of laminar flow for a much larger distance along the surfaces of blunted bodies and wings.

These advantages with regard to increased laminar run and increased laminar stability appear to involve no serious disadvantages. The friction drag is reduced, and the total drag should not increase appreciably for the small required values of the bluntness ratio. Reference 16 shows that, for spherical-tipped cones of fixed total length, the total drag to Mach number 7.0 is very near the value obtained for the sharp-tipped cone for ratios of nose diameter to maximum body diameter less than 0.25.

The quantitative effects of blunting on transition location previously computed are based on the hypothesis that the transition Reynolds number is substantially unchanged when a body with a sharp tip is blunted. Although this hypothesis produces good agreement with the experimental results of reference 3, the possibility should certainly be kept in mind that, at higher Mach numbers or with other body shapes, the transition Reynolds number may be altered by such factors as pressure gradient and outer-edge Mach number and Reynolds number. Furthermore, as the length of laminar run increases, the possibility of premature transition due to surface roughness or stream turbulence also increases, and the dissipation of the shock-produced shear profile becomes important. Whether any of these factors will seriously reduce the attainable downstream movement of transition due to blunting remains to be determined experimentally.

Many theoretical problems also require solution before the quantitative effects of blunting on transition can be predicted with confidence. One basic problem, of course, is that of the development of a laminar boundary layer in a nonuniform external stream. Solution of this problem would establish the magnitude of external shear that is negligible and, consequently, the conditions for which the boundary layer can be assumed to develop in a layer of reduced Reynolds number corresponding to the mean value near the surface. This solution might

reveal whether, as indicated by the results of reference 3, it is sufficient, in general, to obtain the maximum reduction in Reynolds number only for the inner half or two-thirds of the boundary layer rather than at the outer edge. The latter question, however, involves predicting the location of transition for various velocity profiles, which cannot as yet be done even for laminar layers in a uniform external stream. Since the required blunting is small, however, this question appears to be of secondary importance.

CONCLUDING REMARKS

It is clear from the preceding discussion that many questions remain unanswered in this report. The principal observation that the Reynolds number and Mach number near the surface are reduced by blunting, and also the approximate magnitude of the reductions are fairly well established. The assumption that the boundary-layer development should be determined primarily by the reduced Reynolds number and Mach number near the surface rather than by the flow outside the inviscid shear layer also seems reasonable. The principal benefits from blunting, however, lie in the hypersonic speed range, where many of the quantitative results calculated herein are subject to corrections whose magnitude is as yet unknown. Qualitative estimates indicate that some of these corrections, such as the displacement effect or the pressure gradients, either inviscid or self-induced by the boundary layer, should have a favorable effect on the downstream movement of transition. Other effects, such as surface roughness, stream turbulence, or changes in transition Reynolds number, may tend to limit the downstream movement of transition to values less than those predicted. Dissociation at very high Mach numbers may have a significant effect on outer-edge conditions and, consequently, on the maximum transition movement to be expected. As usual, when so many unknown factors contribute to a phenomenon, experiment must be relied upon to determine which factors are dominant and which are of minor importance.

Lewis Flight Propulsion Laboratory
National Advisory Committee for Aeronautics
Cleveland, Ohio, November 21, 1955

APPENDIX A

SYMBOLS

The following symbols are used in this report:

A	area
$(A^*/A)_M$	isentropic area contraction ratio from Mach number M to Mach number 1.0
a	speed of sound
B	$\frac{P_0}{P_C} (A^*/A)_{M_0}$
C	constant in linear viscosity-temperature relation
$C_{p,st}$	stagnation pressure coefficient
c	$\frac{U_0}{r} \sqrt{\frac{\rho_0}{\rho_{st}} C_{p,st}}$
D	$\frac{1 + 0.2M_n^2}{1 + 0.2M_1^2} = \frac{t_1}{t_n}$
$g^*\left(0, \frac{t_w}{t_\infty}, M_\infty\right)$	shear function at surface (ref. 11)
h	heat-transfer coefficient
k	thermal conductivity of air
L	length of conical tip
M	Mach number
Nu	Nusselt number
P	stagnation pressure
p	static pressure

q	heat-transfer rate
Re	Reynolds number
r	recovery factor or radius
r_1	cone radius at station where profiles are determined
S	Sutherland's constant for air, 198.6° R
T	stagnation temperature
t	static temperature
t_w	surface temperature
U	velocity
U_{sp}	velocity downstream of normal shock ahead of spherical nose
x	distance along surface
y	coordinate normal to surface
β	$\sqrt{M_0^2 - 1}$
Γ	$\frac{t_n + S}{t_1 + S}$
γ	ratio of specific heats, 1.40
δ	boundary-layer thickness
δ^*	boundary-layer displacement thickness
η	inclination of sonic line (ref. 7)
θ_c	semivertex angle of cone
θ_w	semivertex angle of wedge
μ	coefficient of viscosity
ν	μ/ρ

ρ	density
τ	shear force at surface
φ	shock angle

Subscripts:

C	centroid
c	cone
e	equilibrium
n	inviscid surface values for blunted cones or wedges
S	sonic point on detached shock wave
SB	sonic point on body
sp	sphere
st	stagnation
tr	transition point
W	wedge
w	surface values
0	ambient conditions
1	inviscid surface values for unblunted cones or wedges
∞	value at outer edge of boundary layer

Superscript:

'	local conditions in inviscid shear layer

APPENDIX B

DISSIPATION OF THE LOW MACH NUMBER LAYER

In order to estimate more closely the amount of blunting required to maintain a given thickness of the low Mach number layer, the rate of dissipation of the shock-produced profile must be considered. The simplest method for estimating the rate is to consider the profile produced by the detached shock wave as a step function (sketch 4):

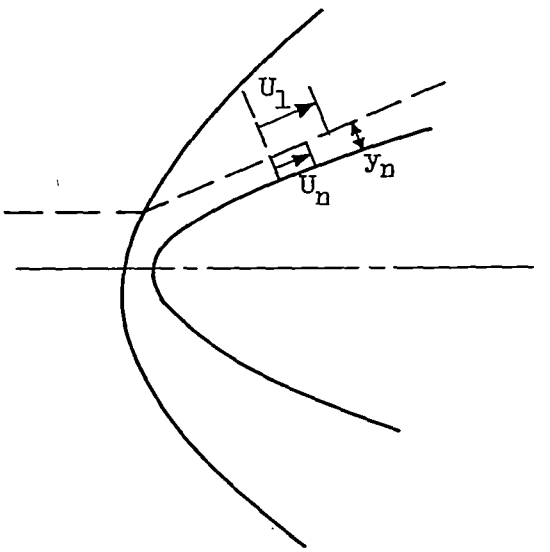

Sketch 4

in which the outer velocity is that corresponding to the unblunted body and the inner velocity is that produced near the surface by blunting the vertex. The profile dissipation can then be considered identical to that at the interface of two parallel laminar jets emerging at the same static pressure. The equation for the velocity profile in the interaction region is given in reference 17 for the case when U_1 and U_n differ by a small amount. The appropriate equation is:

$$\frac{U - U_1}{U_n - U_1} = \frac{1}{2}\left\{\Phi\left[\frac{\left(1 - \frac{y}{y_n}\right)\sqrt{Re_{y_n}}}{2\sqrt{x/y_n}}\right] + \Phi\left[\frac{\left(1 + \frac{y}{y_n}\right)\sqrt{Re_{y_n}}}{2\sqrt{x/y_n}}\right]\right\} \qquad (B1)$$

where y_n is the initial thickness of the low Mach number layer, Re_{y_n} is Reynolds number based on y_n and outer-flow conditions, and $\Phi(\alpha)$ is the error function of α. Profiles calculated from equation (B1) for

$Re_{y_n} = 10^4$ and for several values of x/y_n are shown in figure 8. Apparently, the velocity near the surface does not change appreciably until x/y_n is of the order of 1000. Although these profiles are valid only for small differences between U_1 and U_n, the order of magnitude of the dissipation remains the same for large differences (see fig. 4.11, ref. 17). The value of $x/y_n < 1000$ is, therefore, probably a good estimate for the length of run in which dissipation of the shock-produced shear profile can be neglected if this profile remains laminar.

If transition to turbulence takes place in this layer, the length of run for which dissipation can be neglected is appreciably reduced. No experimental results are available to estimate under what conditions the shock-produced shear profile is likely to undergo transition. However, an indication of whether transition is a possibility in this layer can be obtained from the stability criterion for parallel jets developed in reference 18. This criterion states that the interface can become unstable if the quantity $\frac{\partial}{\partial y}\left(\rho \frac{\partial u}{\partial y}\right)$ vanishes in the interface profile. However, the profile is stable if this quantity vanishes only at points in the profile where the velocity satisfies one or both of the following inequalities:

$$U < U_1 - a_1$$

$$U > U_n + a_n$$

These conditions assure that disturbances from either stream will not reach a layer in which amplification is possible.

In terms of Mach number profiles, these conditions can be stated as follows:

The profile is stable to two-dimensional disturbances if the quantity $\frac{d}{dy}\left\{\frac{dM/dy}{\sqrt{1 + \frac{\gamma - 1}{2} M^2}}\right\}$ vanishes only at points where

$$M < \frac{M_1 - 1}{\sqrt{(\gamma - 1)(M_1 + 2)}} \tag{B2}$$

or where

$$M > \frac{M_n + 1}{(\gamma - 1)(2 - M_n)} \tag{B3}$$

The latter condition cannot be satisfied for $M_n \geq 2.0$. Consequently, the stability of the profile depends chiefly on whether $\frac{d}{dy}\left[\frac{dM/dy}{1 + \frac{\gamma - 1}{2} M^2}\right]$ vanishes only where condition (B2) is fulfilled. Some sample computations based on the profiles of figure 4 indicate that condition (B2) is generally satisfied for the blunted-cone profile but not for the blunted-wedge profiles. The latter profiles therefore are more inclined to undergo transition than the former. If transition occurs, the amount of bluntness required to produce a prescribed thickness of the low Mach number layer at a given station may be considerably greater than calculated on the basis of laminar flow. This discussion must necessarily be inconclusive, since the location or even the existence of transition cannot be established from stability theory alone.

APPENDIX C

MACH NUMBER PROFILES PRODUCED BY DETACHED SHOCK WAVES

The Mach number profiles normal to the surfaces of cones and wedges with slightly blunted tips or leading edges can be calculated from the one-dimensional continuity equation if (1) the form and location of the detached shock wave is known, (2) the static pressure is constant normal to the surface, and (3) diffusion and dissipation of the profile are neglected. Condition (1) is most conveniently satisfied by using the detached-shock-wave theory of reference 7. Condition (2) is satisfied at stations sufficiently far downstream of the nose or leading edge, where the surface static pressure has reached, or closely approached, the value obtained with unblunted cones or wedges. At moderate supersonic Mach numbers, the required distance is of the order of 3 to 10 times the thickness of the blunted portion of the nose or leading edge. This condition is not quite satisfied for blunted cones, because the flow field approaches a conical distribution characterized by a gradual decrease of static pressure from the surface to the shock wave. But if the profile extends only a small portion of the distance from the surface to the shock wave, this gradient can be neglected without serious error. Condition (3) remains an assumption whose validity decreases as the distance along the body increases. It implies that the profile remains unchanged in form for an unlimited distance downstream of the vertex. As pointed out in appendix B, this assumption appears to be fairly good for distances of the order of 1000 times the thickness of the blunted portion of the body if the profile remains laminar.

The profile computation is set up with the aid of sketch 5, which

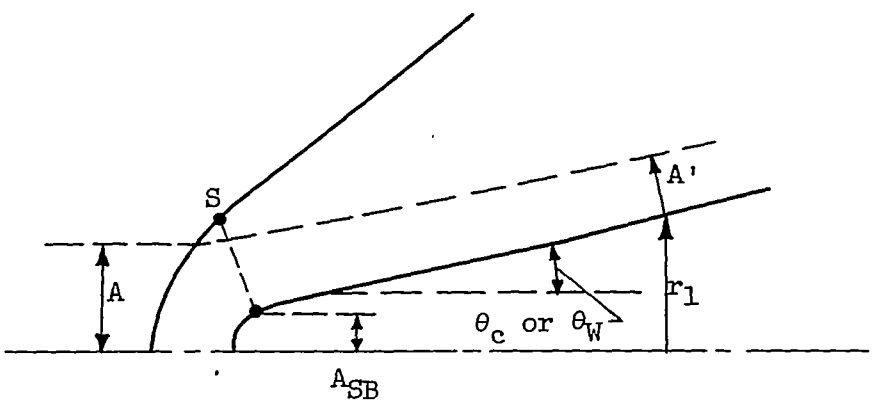

Sketch 5

applies either for cones or wedges. If the sonic-point area of the body is used for reference purposes, the continuity equation can be written as

$$\frac{A'}{A_{SB}} = \int_0^{A/A_{SB}} \frac{\rho_0 U_0}{\rho' U'} \, d\left(\frac{A}{A_{SB}}\right) \tag{C1}$$

or

$$\frac{A'}{A_{SB}} = \int_0^{A/A_{SB}} \frac{P_0}{P'} \frac{(A^*/A)_{M_0}}{(A^*/A)_{M'}} \, d\left(\frac{A}{A_{SB}}\right) \tag{C2}$$

where the primes refer to local conditions in the inviscid shear layer. Since the stagnation pressure along each streamline remains constant downstream of the shock, P'/P_0 is the stagnation-pressure ratio across the shock at the point where the streamline bounding the area A enters the shock. If the shock angle at this point is φ, then the total-pressure ratio can be written (ref. 19)

$$\frac{P'}{P_0} = \left(\frac{6M_0^2 \sin^2\varphi}{M_0^2 \sin^2\varphi + 5}\right)^{7/2} \left(\frac{6}{7M_0^2 \sin^2\varphi - 1}\right)^{5/2} \tag{C3}$$

The Mach number M' at the area A' can also be expressed in terms of shock angle by the relation

$$1 + 0.2M'^2 = \left(\frac{P'}{p_1}\right)^{\frac{\gamma-1}{\gamma}} \equiv \left(\frac{P'}{P_0} \frac{P_0}{p_0} \frac{p_0}{p_1}\right)^{2/7} \tag{C4}$$

The function $(A^*/A)_{M'}$, as well as P'/P_0, is a function of the shock angle φ at the point where the streamline crosses the shock wave. The differential $d(A/A_{SB})$ of equation (C2) must be converted into a function of φ in order that the integration may be carried out from $\varphi = 90^\circ$ to $\varphi = \varphi_1$, where φ_1 is the shock angle corresponding to the unblunted cone or wedge. The Mach number M' as a function of A' can then be obtained from equations (C4) and (C3).

From reference 7 (eq. (5)), the relation between shock angle and shock ordinate for the assumed hyperbolic wave is

$$\left(\frac{y}{y_{SB}}\right)^2 = \frac{(x_0/y_{SB})^2}{\beta^2(\beta^2\tan^2\varphi - 1)} \tag{C5}$$

where

$$\frac{x_0}{y_{SB}} = \beta \frac{y_S}{y_{SB}} \sqrt{\beta^2\tan^2\varphi_S - 1} \tag{C6}$$

and φ_S is the shock angle at the shock sonic point. The ratio y_S/y_{SB} is a function of M_0 and depends on whether the flow is two-dimensional or axially symmetric.

The area differential of equation (C2) can now be expressed as follows:

For two-dimensional flow:

$$d\left(\frac{A}{A_{SB}}\right) \equiv d\left(\frac{y}{y_{SB}}\right) = -\beta \frac{x_0}{y_{SB}} \left[\frac{\tan\varphi \sec^2\varphi \, d\varphi}{(\beta^2\tan^2\varphi - 1)^{3/2}}\right] \tag{C7}$$

For axially symmetric flow:

$$d\left(\frac{A}{A_{SB}}\right) \equiv d\left(\frac{y}{y_{SB}}\right)^2 = -2\left(\frac{x_0}{y_{SB}}\right)^2 \left[\frac{\tan\varphi \sec^2\varphi \, d\varphi}{(\beta^2\tan^2\varphi - 1)^2}\right] \tag{C8}$$

Combination of equations (C2) to (C8) yields the following final expressions for determining the variation of M' with A':

For plane flow:

$$\frac{A'}{A_{SB}} \equiv \frac{y'}{y_{SB}} = -\beta^2 \frac{y_S}{y_{SB}} \sqrt{\beta^2\tan^2\varphi_S - 1} \frac{p_0}{p_1} \int_{90^\circ}^{\varphi} \left(\frac{1 + 0.2M_0^2}{1 + 0.2M'^2}\right)^{1/2} \frac{M_0}{M'} \left(\frac{\tan\varphi \sec^2\varphi}{(\beta^2\tan^2\varphi - 1)^{3/2}}\right) d\varphi \tag{C9}$$

For axially-symmetric flow:

$$\frac{A'}{A_{SB}} = -2\beta^2\left(\frac{y_S}{y_{SB}}\right)^2\left(\beta^2\tan^2\varphi_S - 1\right)\frac{p_0}{p_1}\int_{90^\circ}^{\varphi}\left(\frac{1 + 0.2M_0^2}{1 + 0.2M'^2}\right)^{1/2}\frac{M_0}{M'}\left(\frac{\tan\varphi\,\sec^2\varphi}{(\beta^2\tan^2\varphi - 1)^2}\right)d\varphi \qquad \text{(C10)}$$

In these equations, y' is the linear distance normal to the wedge or cone. For $y' \ll r_1$, the area ratio A'/A_{SB} in equation (10) is equal to $\frac{2r_1y'}{y_{SB}^2}$.

Equations (C9) and (C10) have been integrated numerically for several Mach numbers and for several wedge and cone angles. The resulting Mach number profiles are shown in figure 4.

3880

REFERENCES

1. Brinich, Paul F., and Diaconis, Nick S.: Boundary-Layer Development and Skin Friction at Mach Number 3.05. NACA TN 2742, 1952.

2. Dunning, Robert W., and Ulmann, Edward F.: Effects of Sweep and Angle of Attack on Boundary-Layer Transition on Wings at Mach Number 4.04. NACA TN 3473, 1955.

3. Brinich, Paul F.: Effect of Leading-Edge Geometry on Boundary-Layer Transition at Mach 3.1. NACA TN 3659, 1956.

4. Ferri, Antonio, and Libby, Paul A.: Note on an Interaction Between the Boundary Layer and the Inviscid Flow. Jour. Aero. Sci., vol. 21, no. 2, Feb. 1954, p. 130.

5. Lees, Lester: Hypersonic Flow. Preprint No. 554, Inst. Aero. Sci., June 1955.

6. Dorrance, William H., and Romig, Mary F.: The Effect of Blunting the Nose of a Cone on Conical Surface Reynolds Number and Laminar Flow Heat Transfer at Hypersonic Mach Numbers. Rep. ZA-7-015, Consolidated Vultee Aircraft Corp., Mar. 11, 1955.

7. Moeckel, W. E.: Approximate Method for Predicting Form and Location of Detached Shock Waves Ahead of Plane or Axially Symmetric Bodies. NACA TN 1921, 1949.

8. Moeckel, W. E.: Experimental Investigation of Supersonic Flow with Detached Shock Waves for Mach Numbers Between 1.8 and 2.9. NACA RM E50D05, 1950.

9. Low, George M.: The Compressible Laminar Boundary Layer with Fluid Injection. NACA TN 3404, 1955.

10. Chapman, Dean R., and Rubesin, Morris W.: Temperature and Velocity Profiles in the Compressible Laminar Boundary Layer with Arbitrary Distribution of Surface Temperature. Jour. Aero. Sci., vol. 16, no. 9, Sept. 1949, pp. 547-565.

11. Van Driest, E. R.: Investigation of Laminar Boundary Layer in Compressible Fluids Using the Crocco Method. NACA TN 2597, 1952.

12. Romig, Mary F., and Dore, F. J.: Solutions of the Compressible Laminar Boundary Layer Including the Case of a Dissociated Free Stream. Rep. ZA-7-012, San Diego Div., Convair, Aug. 1954.

13. Dunn, D. W., and Lin, C. C.: Of the Stability of the Laminar Boundary Layer in a Compressible Fluid. Jour. Aero. Sci., vol. 22, no. 7, July 1955, pp. 455-477.

14. Reshotko, Eli, and Cohen, Clarence B.: Heat Transfer at the Forward Stagnation Point of Blunt Bodies. NACA TN 3513, 1955.

15. Cohen, Clarence B., and Reshotko, Eli: The Compressible Laminar Boundary Layer with Heat Transfer and Arbitrary Pressure Gradient. NACA TN 3326, 1955.

16. Sommer, Simon C., and Stark, James A.: The Effect of Bluntness on the Drag of Spherical-Tipped Truncated Cones of Fineness Ratio 3 at Mach Numbers 1.2 to 7.4. NACA RM A52B13, 1952.

17. Pai, Shih-I.: Fluid Dynamics of Jets. D. Van Nostrand Co., Inc., 1954.

18. Lin, C. C.: On the Stability of the Laminar Mixing Region Between Two Parallel Streams in a Gas. NACA TN 2887, 1953.

19. Ames Research Staff: Equations, Tables, and Charts for Compressible Flow. NACA Rep. 1135, 1953. (Supersedes NACA TN 1428.)

(a) Cones.

(b) Wedges.

Figure 1. - Inviscid surface Mach number for blunted cones and wedges.

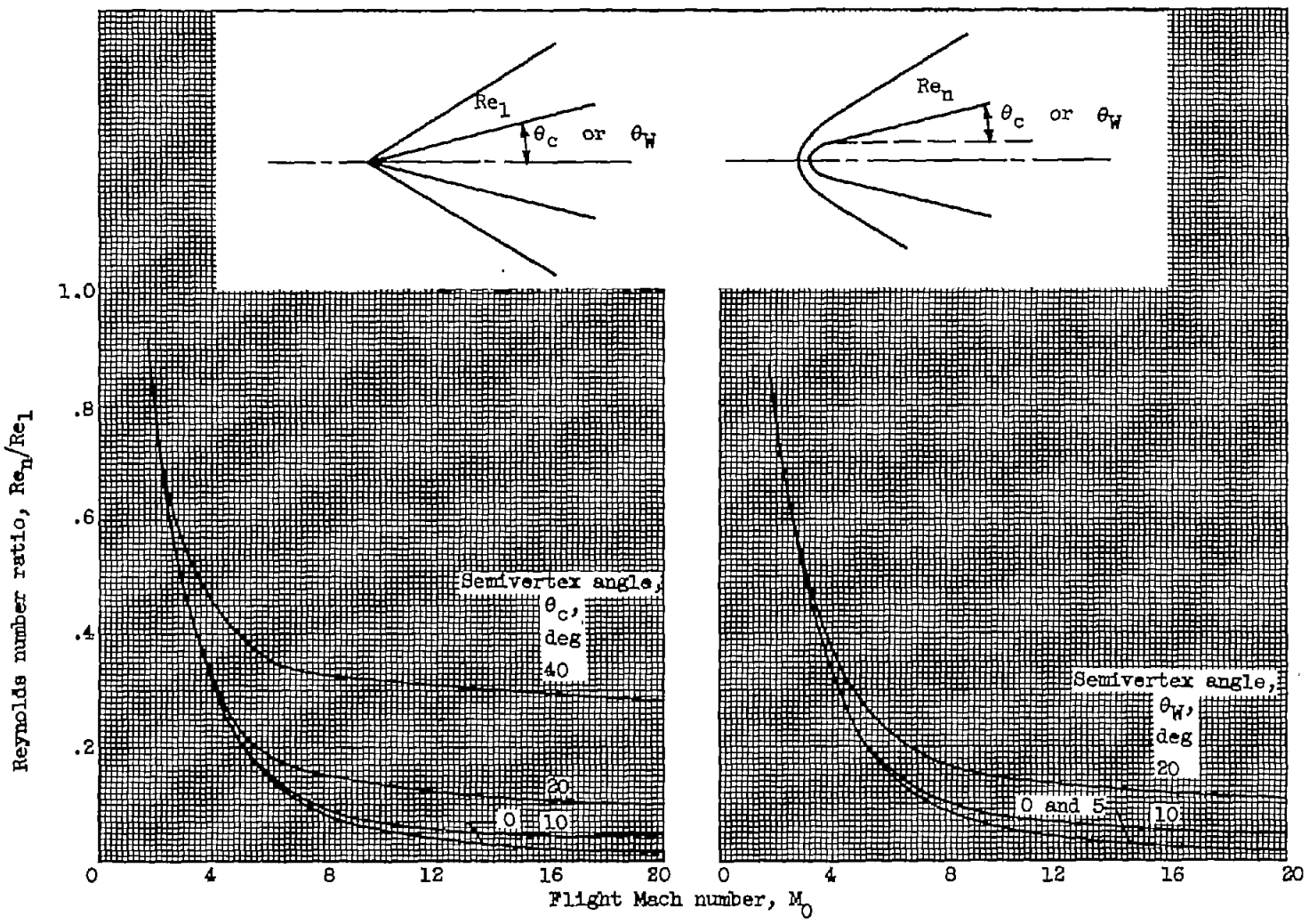

(a) Cones. (b) Wedges.

Figure 2. - Effect of blunting on Reynolds number near surface of cones and wedges. Ambient static temperature, 392.4° R.

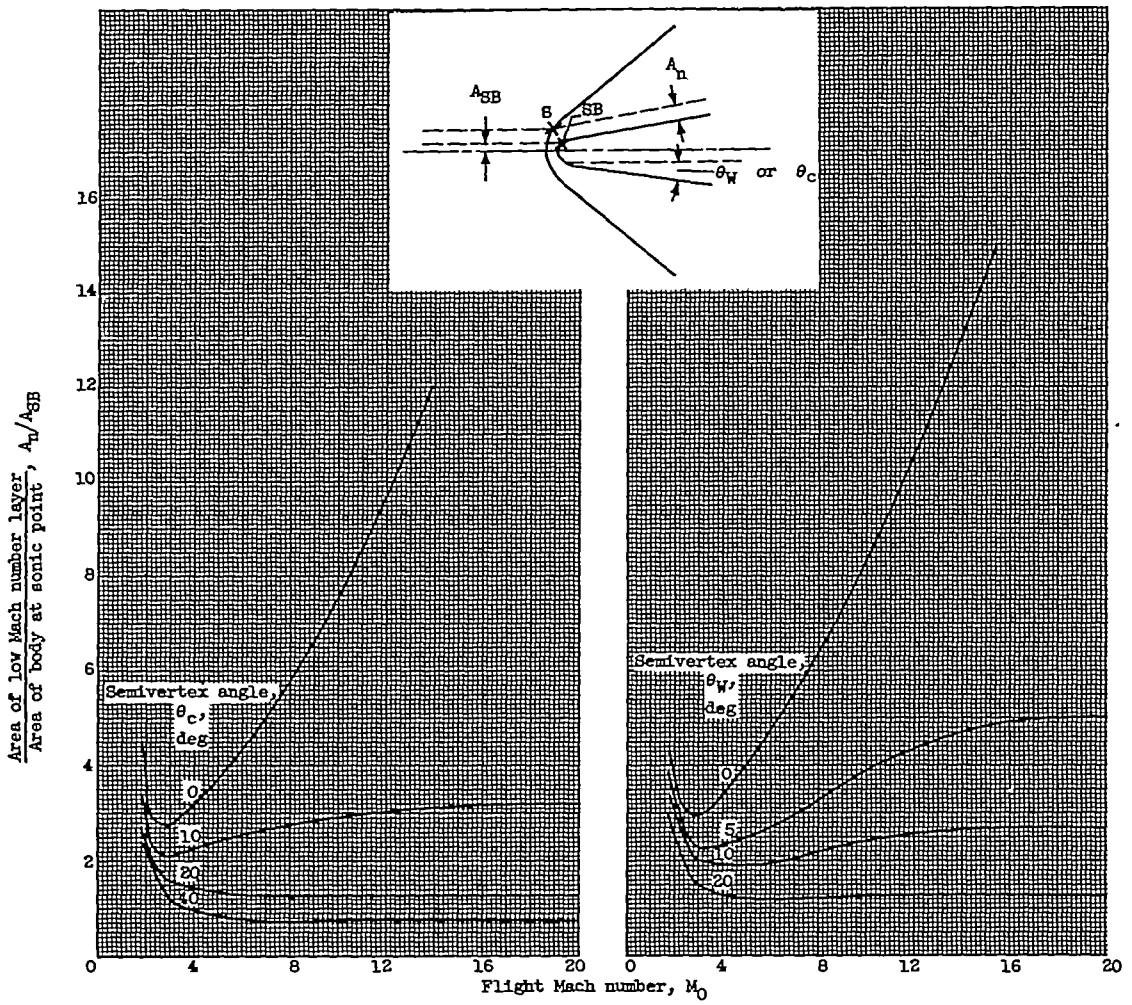

Figure 3. - Area of low Mach number layer for blunted cones and wedges.

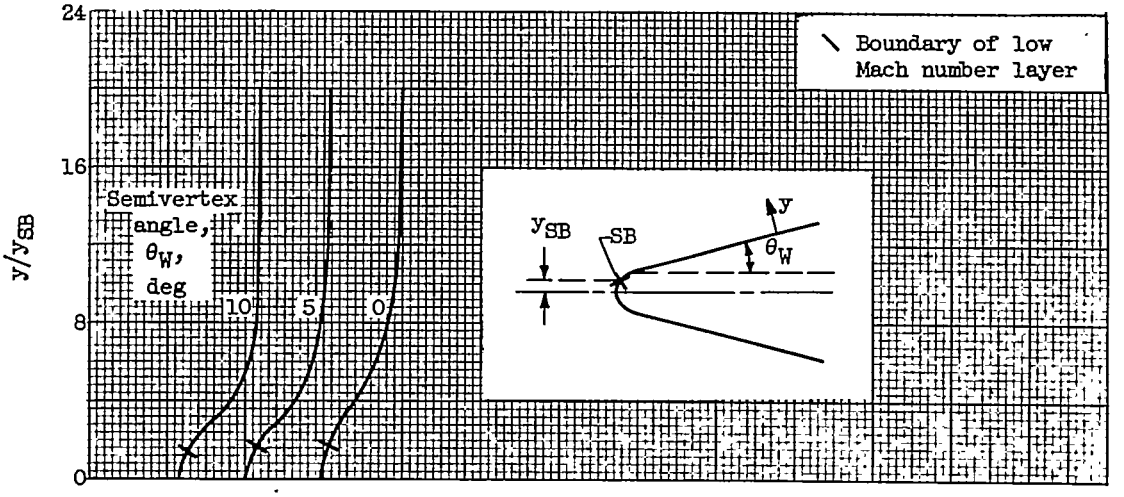

(a) Flight Mach number, 2.0; wedges.

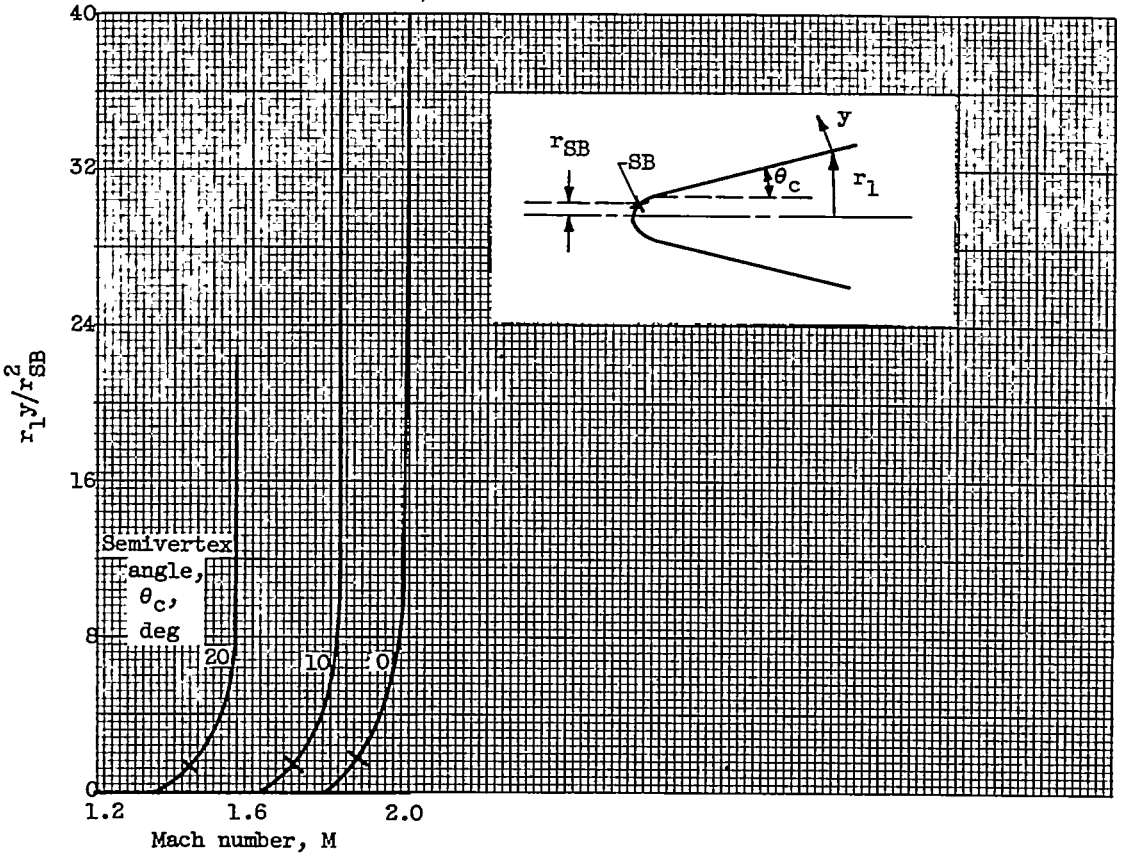

(b) Flight Mach number, 2.0; cones.

Figure 4. - Inviscid Mach number profiles for blunted cones and wedges.

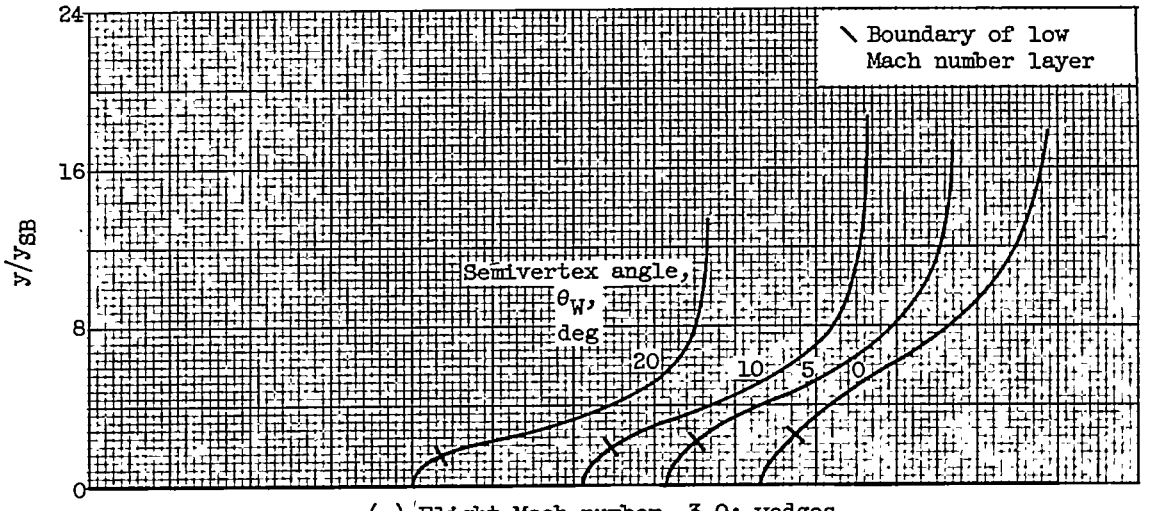

(c) Flight Mach number, 3.0; wedges.

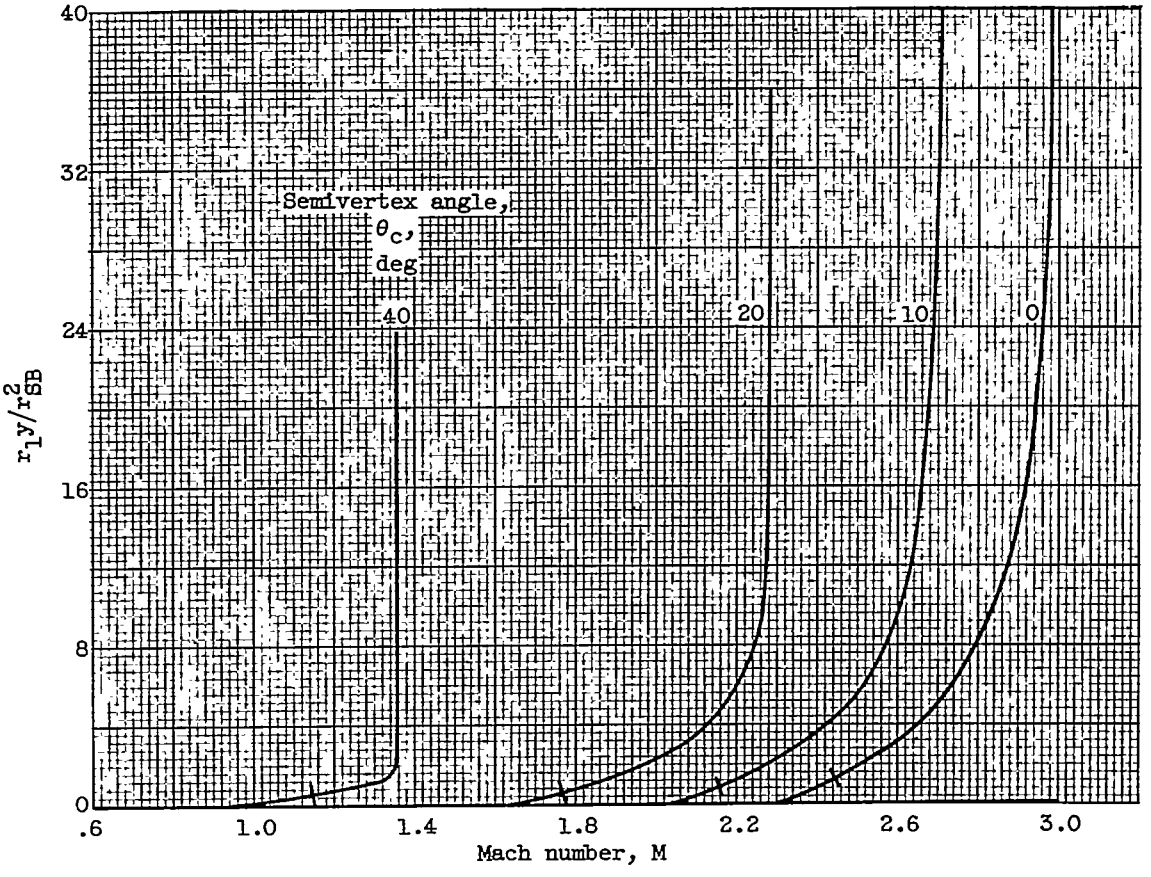

(d) Flight Mach number, 3.0; cones.

Figure 4. - Continued. Inviscid Mach number profiles for blunted cones and wedges.

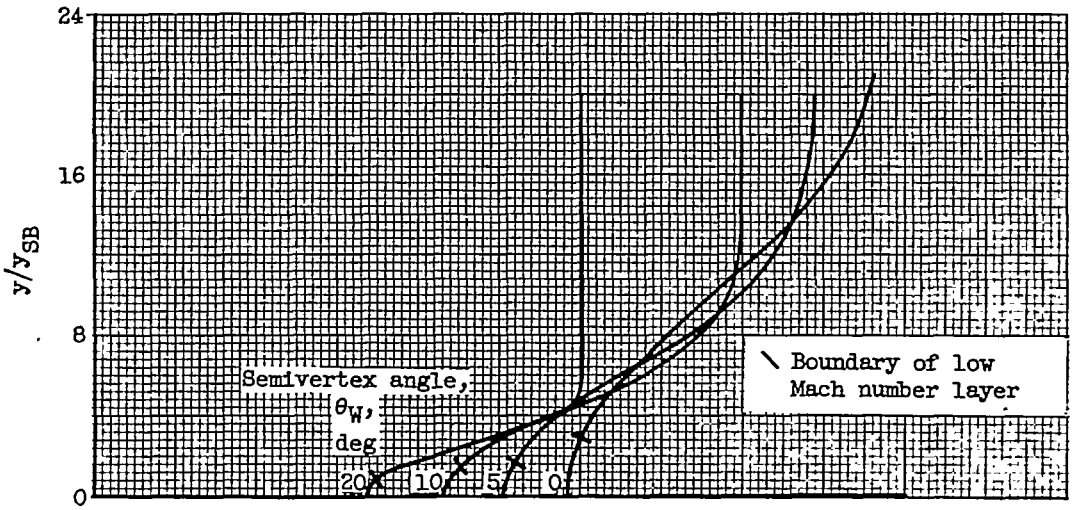

(e) Flight Mach number, 5.0; wedges.

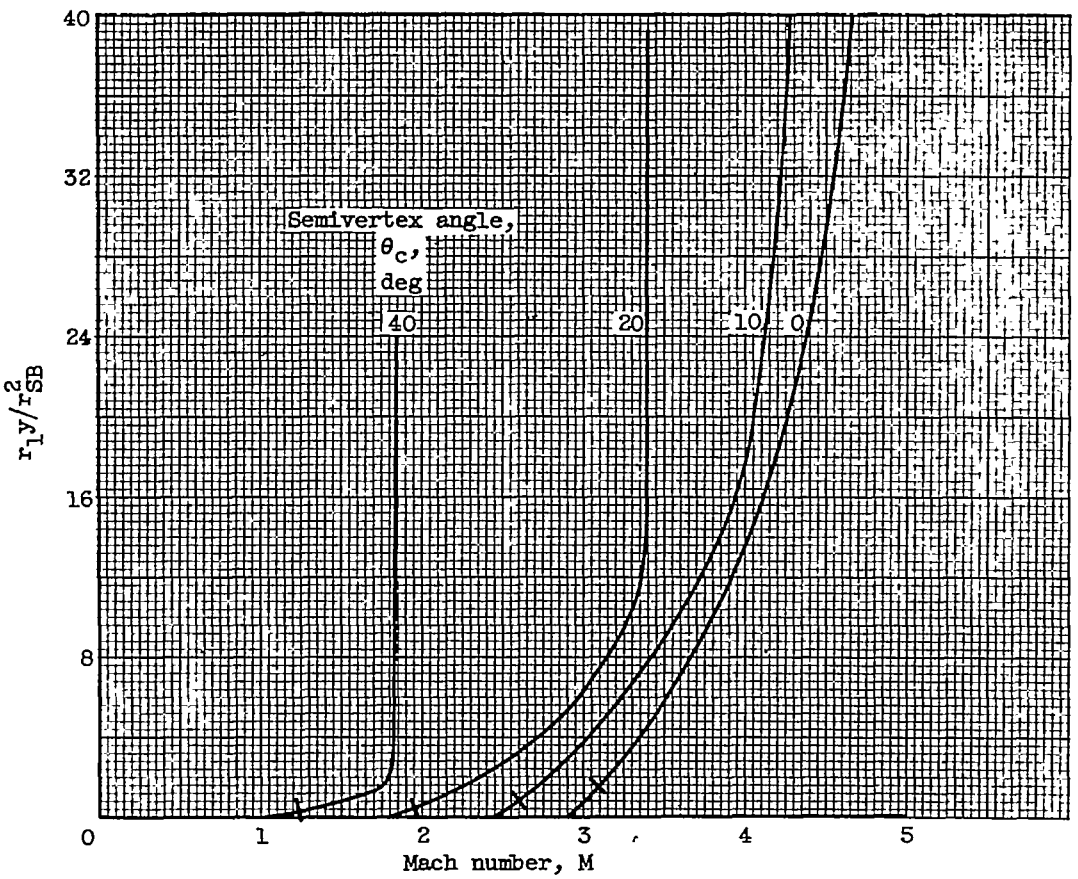

(f) Flight Mach number, 5.0; cones.

Figure 4. - Continued. Inviscid Mach number profiles for blunted cones and wedges.

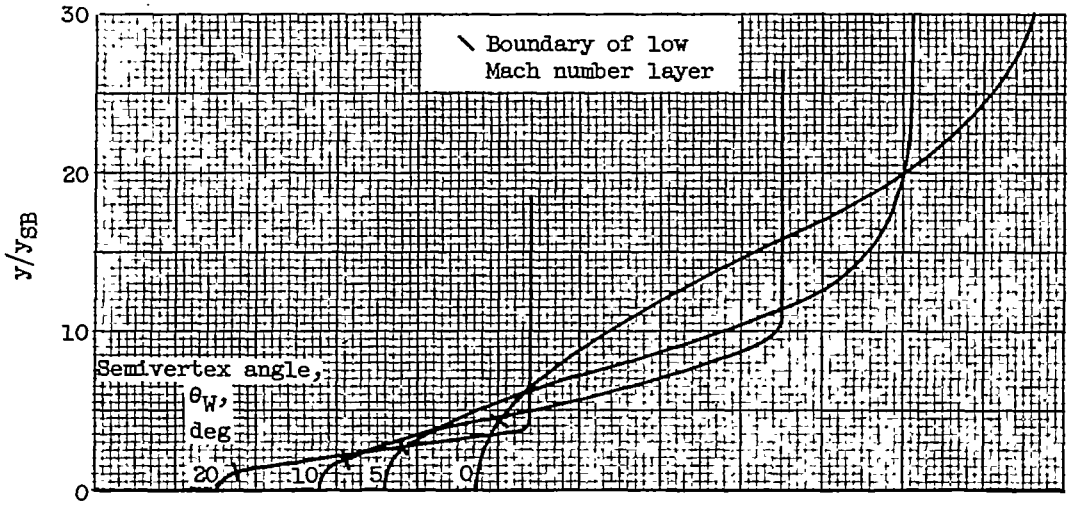

(g) Flight Mach number, 7.0; wedges.

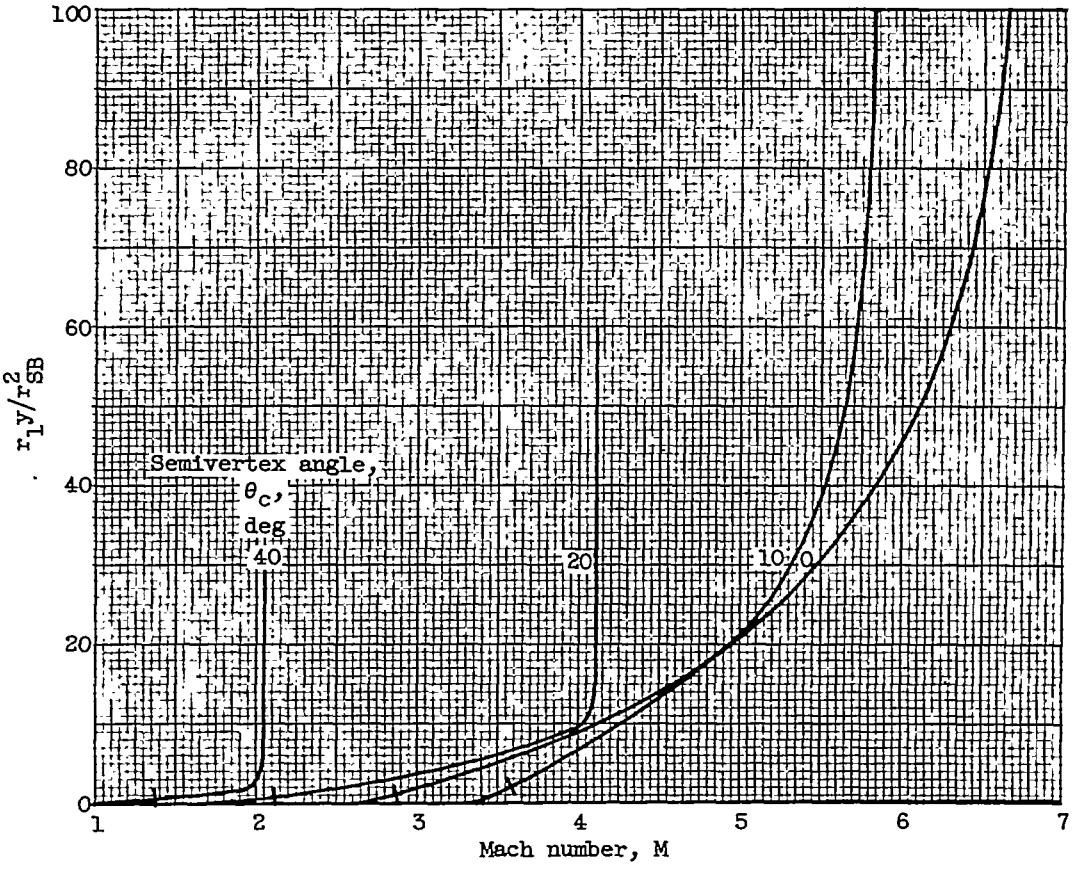

(h) Flight Mach number, 7.0; cones.

Figure 4. - Continued. Inviscid Mach number profiles for blunted cones and wedges.

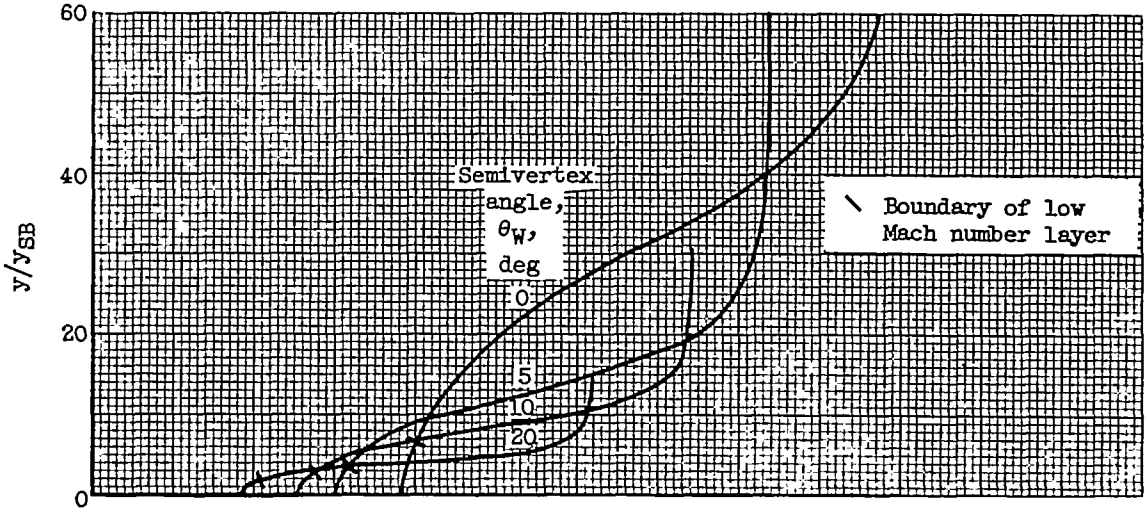

(i) Flight Mach number, 10.0; wedges.

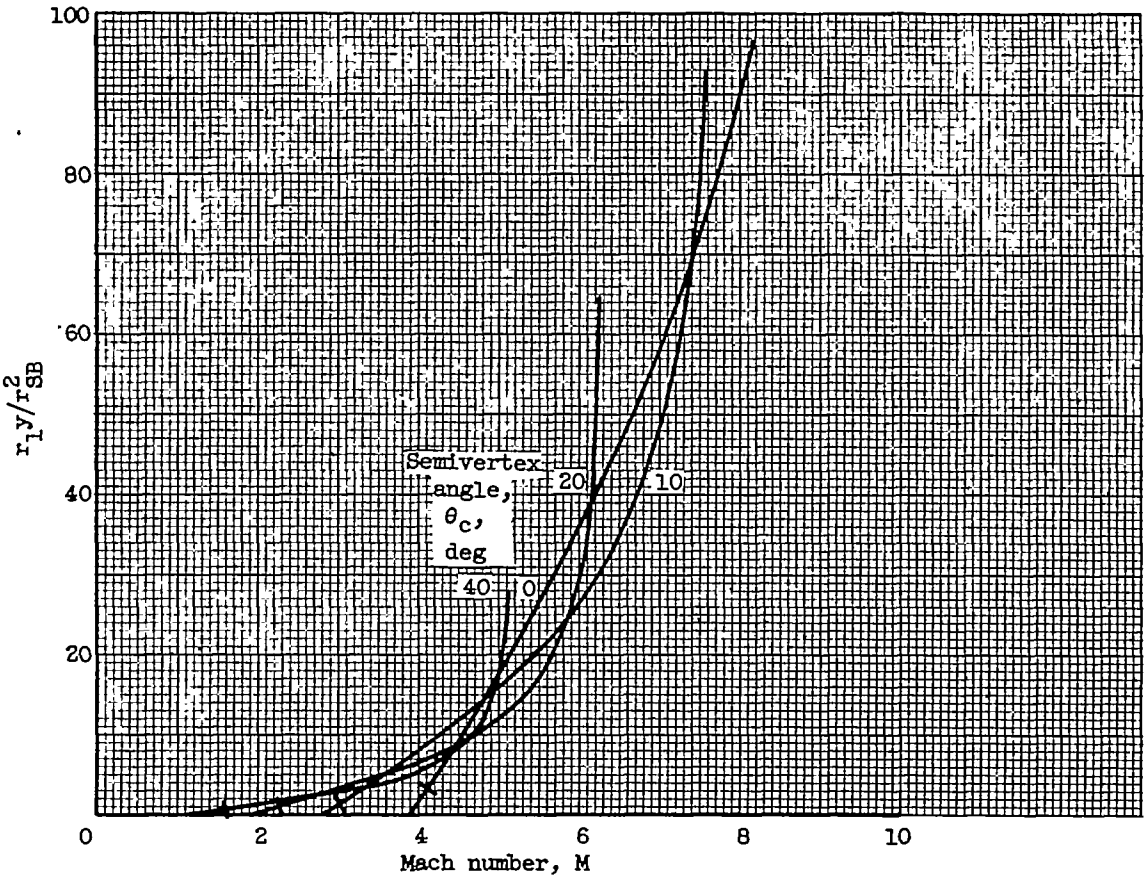

(j) Flight Mach number, 10.0; cones.

Figure 4. - Continued. Inviscid Mach number profiles for blunted cones and wedges.

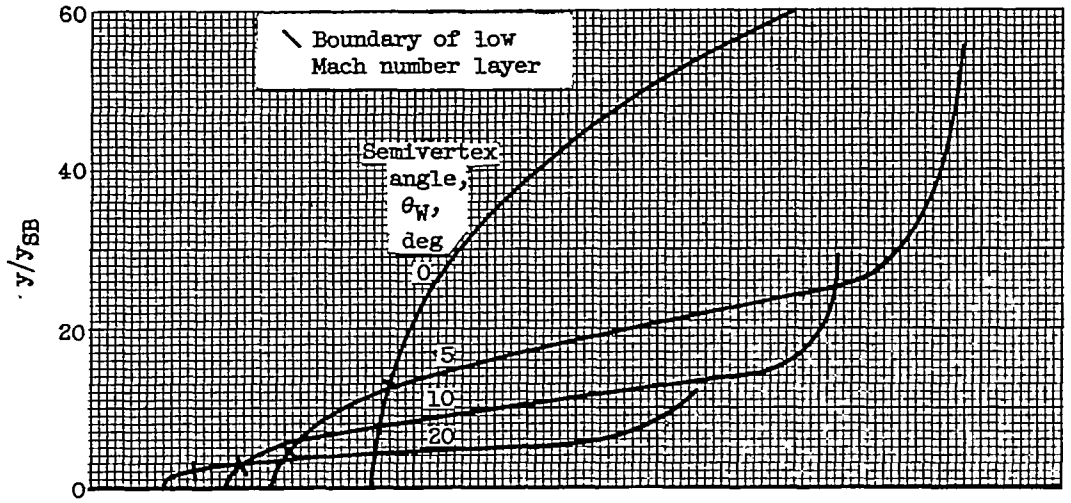

(k) Flight Mach number, 15.0; wedges.

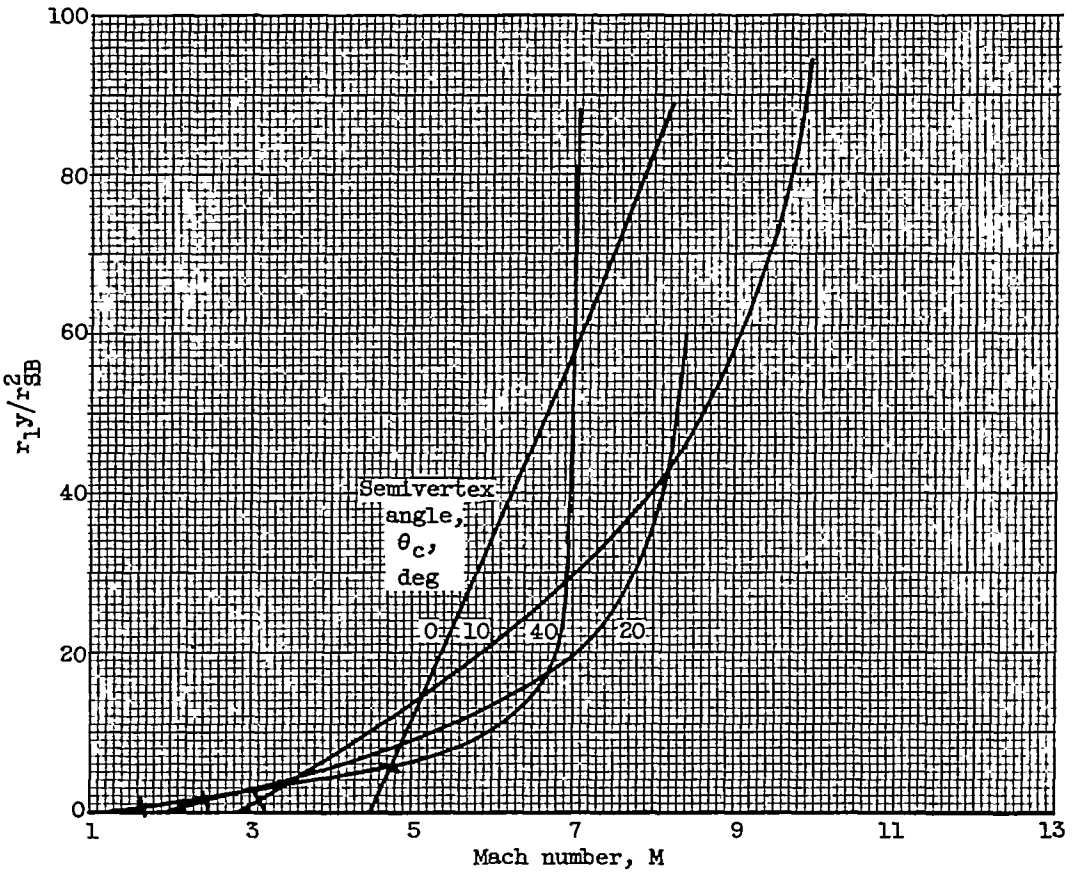

(l) Flight Mach number, 15.0; cones.

Figure 4. - Continued. Inviscid Mach number profiles for blunted cones and wedges.

3880

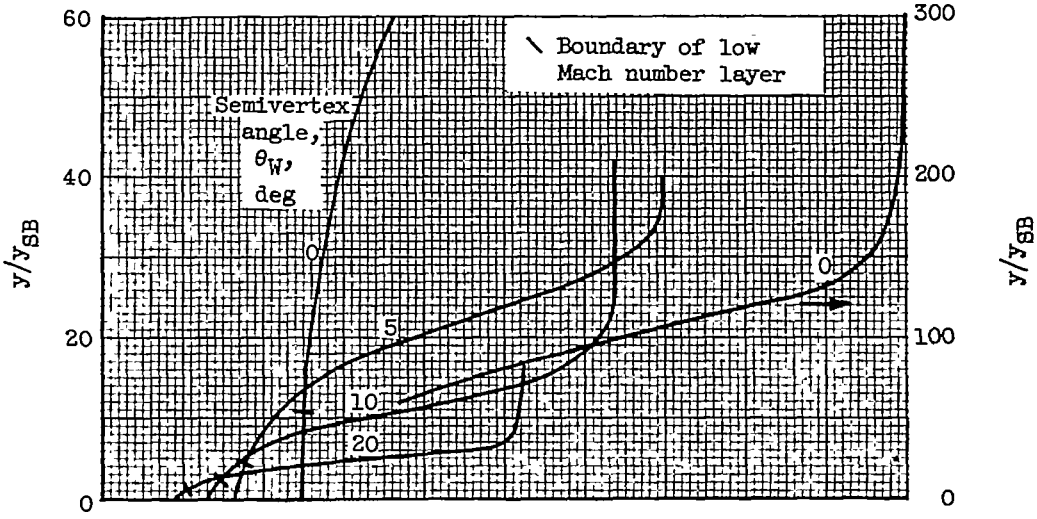

(m) Flight Mach number, 20.0; wedges.

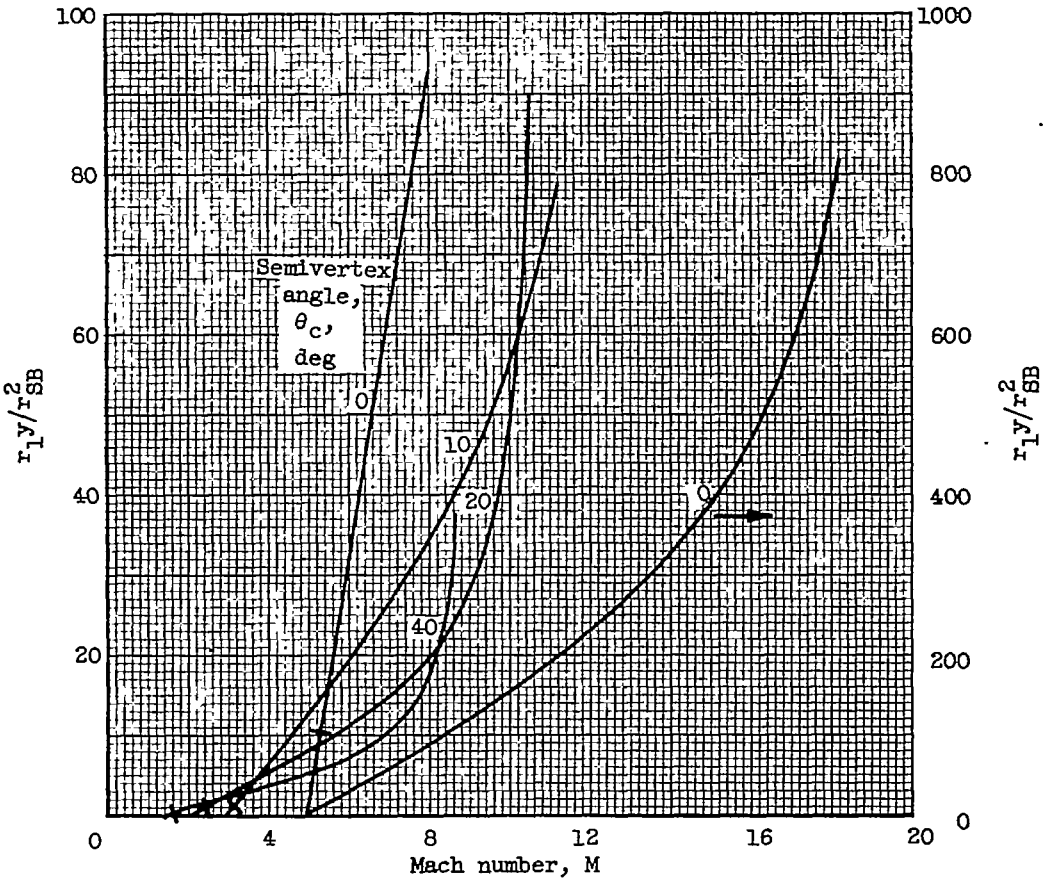

(n) Flight Mach number, 20.0; cones.

Figure 4. - Concluded. Inviscid Mach number profiles for blunted cones and wedges.

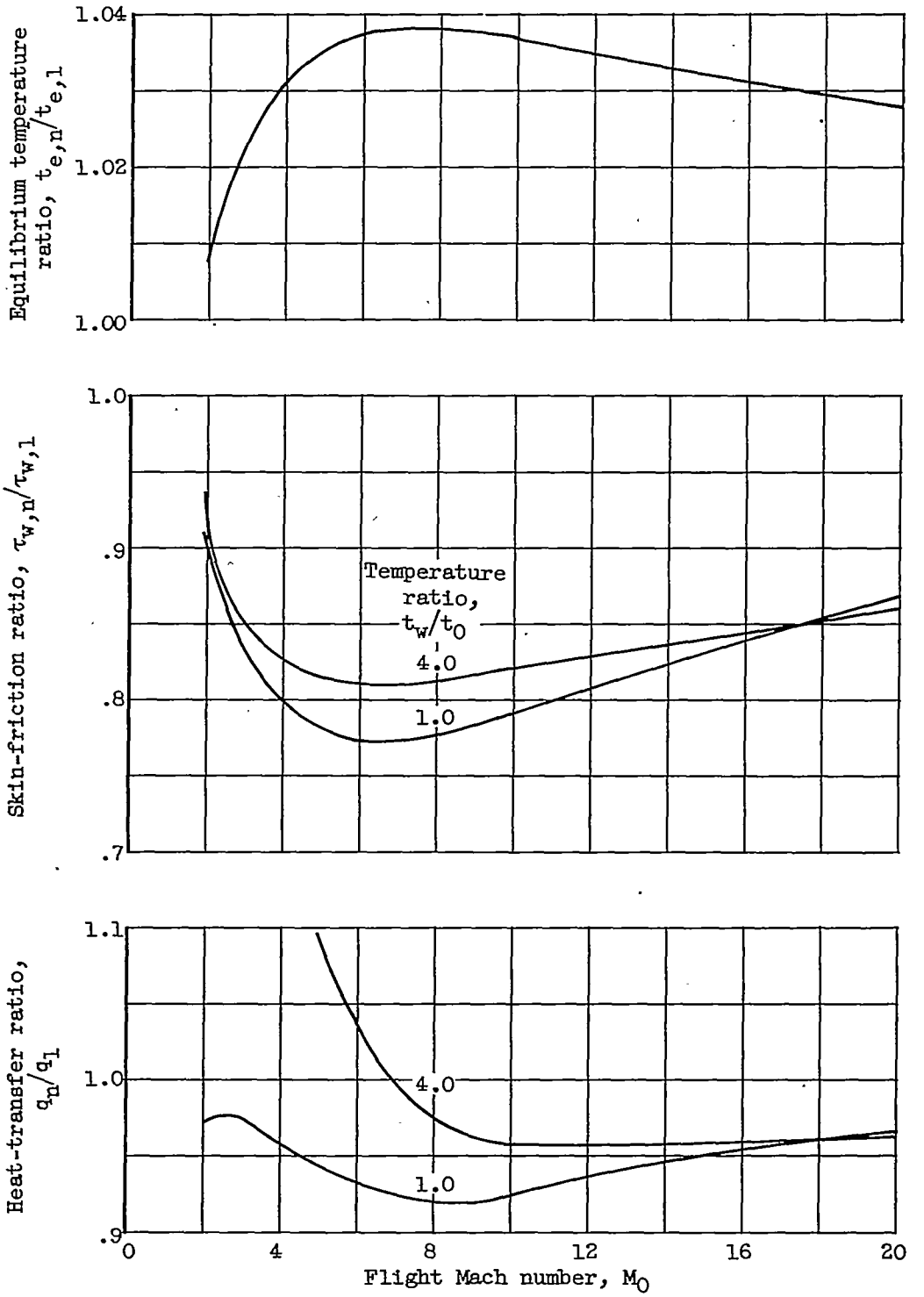

Figure 5. - Effect of blunting on laminar-heat-transfer rate, skin friction, and equilibrium temperature.

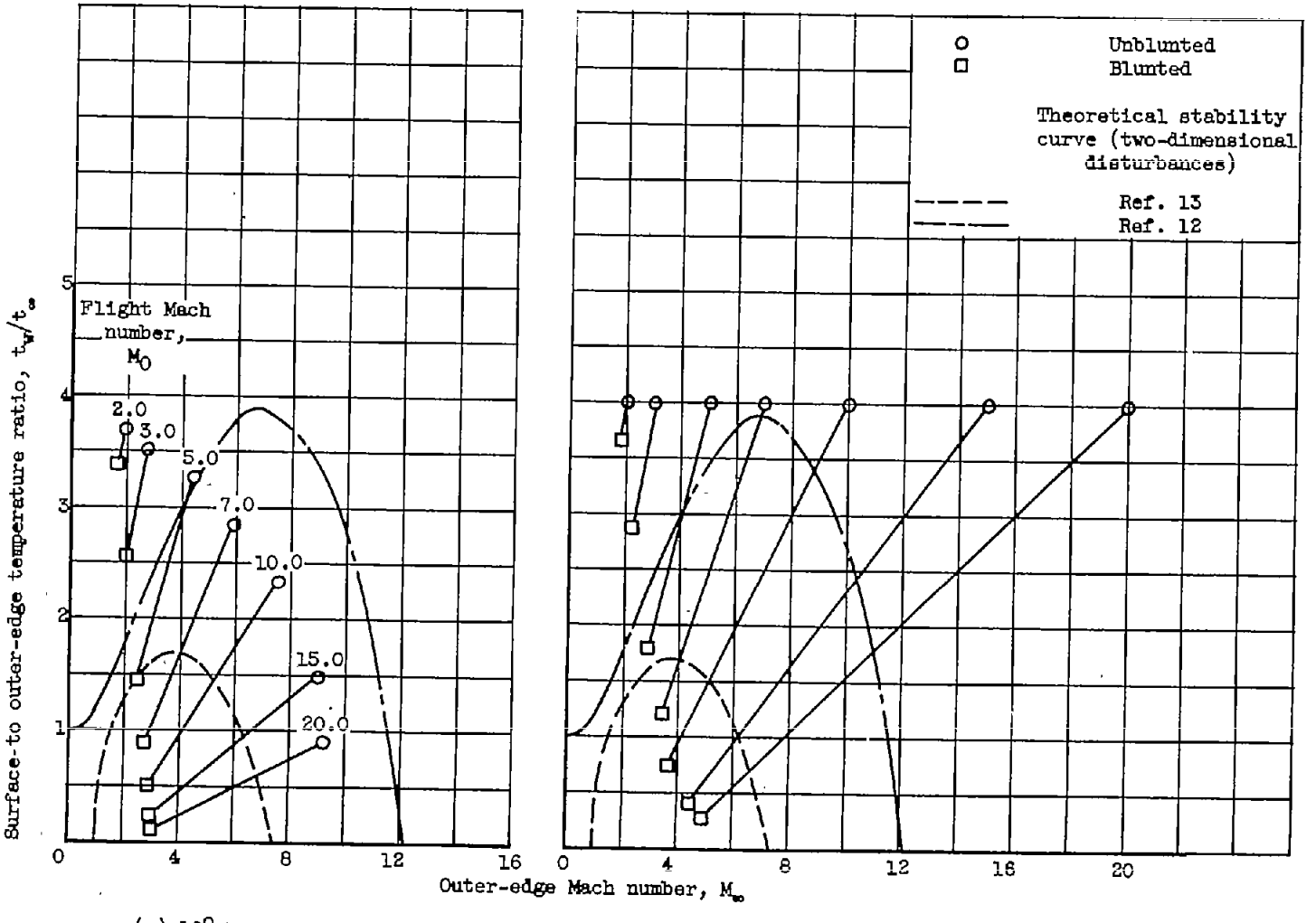

(a) 10° Half-angle cone.

(b) Flat plate.

Figure 6. - Effect of blunting on stability parameters for flat plate and 10° half-angle cone. Surface-to-ambient temperature ratio, 4.0.

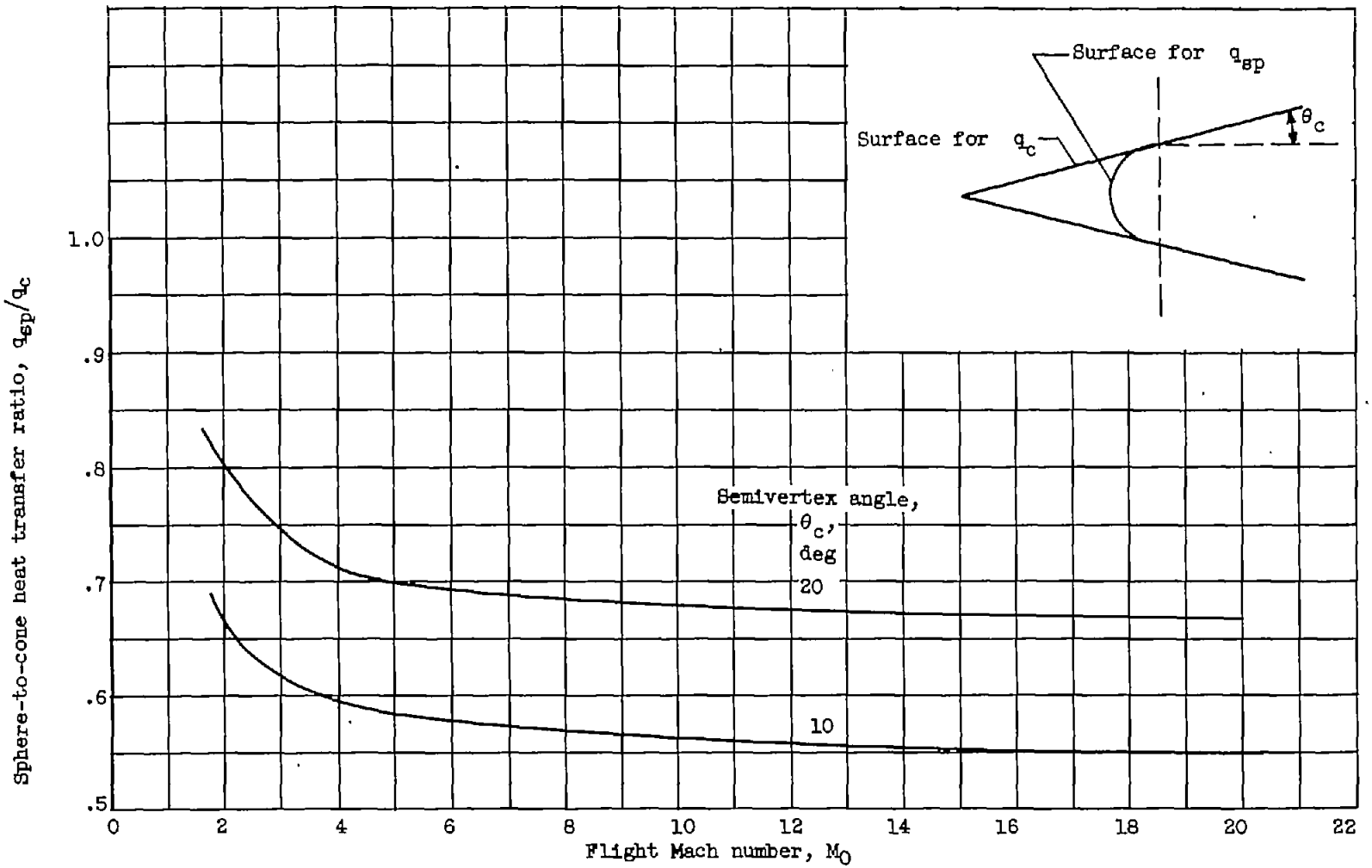

Figure 7. - Comparison of laminar-heat-transfer ratios for spherical and conical noses. Surface-to-ambient static-temperature ratio, 1.0.

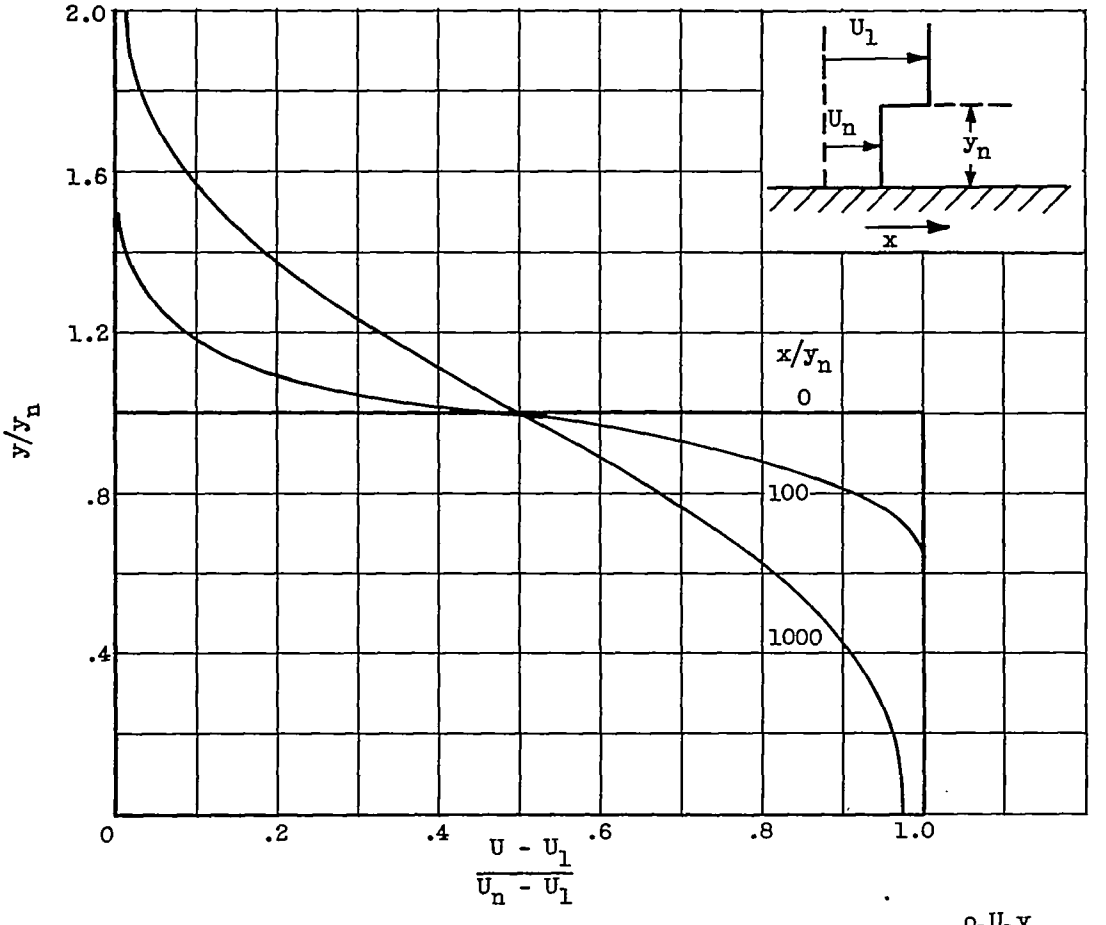

Figure 8. - Laminar diffusion of step velocity profile. $Re_{y_n} \equiv \frac{\rho_l U_l y_n}{\mu_l} = 10^4$